CNIC-00492
CNDC-0005
INDC(CPR)-019/L

# COMMUNICATION OF NUCLEAR DATA PROGRESS

No 4 (1990)



China Nuclear Information Center
Chinese Nuclear Data Center
Atomic Energy Press

CNIC-00492
CNDC-0005
INDC(CPR)-019/L

# COMMUNICATION OF NUCLEAR DATA PROGRESS

No. 4(1990)

Chinese Nuclear Data Center

China Nuclear Information Centre
Atomic Energy Press

Beijing. 1990. 12

# EDITORIAL NOTE

This is the fourth issue of 《 Communication of Nuclear Data Progress》 (CNDP), in which the achievements in nuclear data up to now in China are carried. It includes measurements of neutron small angle scattering cross sections for Fe, Ni and Cr; n–D scattering phase–shift and $^{17}O$ R–Matrix analyses, calculations of neutron elastic and inelastic scattering from $^{7}Li$; evaluations of $^{2}H(n,2n)$, $^{23}Na$, $^{59}Co(n,\gamma)$, $^{235,238}U$, $^{239}Pu(n,f)$ and $(n,\gamma)$ cross sections; and a fitting code of corrected SLBW with multilevel effect (CBNFIT), R–Matrix analysis code (RAC) etc.

We hope that our readers and colleagues will not spare their comments, in order to improve the publication.

Please write to Drs. Liu Tingjin and Zhuang Youxiang.
Mailling Address : Chinese Nuclear Data Center
China Institute of Atomic Energy
P. O. Box 275 (41), Beijing 102413
People's Republic of China
Telephone : 868221 Ext. 2830 or 2729
Telex : 222373 IAE CN.

# CONTENTS

## III DATA EVALUATION



## IV DATA PROCESSING

# I EXPERIMENTAL MEASUREMENT

## SMALL ANGLE SCATTERING CROSS SECTIONS OF 14.8 MeV NEUTRON FOR Fe, Ni AND Cr

Qi Huiquan Chen Hongbing Chen Qiankun
Chen Yingting Chen Zhenpeng Chen Zemin

(TSINGHUA UNIVERSITY)

Fe, Ni and Cr are the important structural material nuclides for fusion application. There is a forword peak in the angular distribution for about 14 MeV neutron. So the precision of the differential scattering cross sections at small angle region has strong influence on the total scattering cross section. The experimental data of scattering cross sections at small angle are very scarce for Fe and Ni and have not published yet for Cr.

The measurements of the small angle scattering cross section in the past several years in Tsinghua University have been reported in Refs.[1～4]. The main detector is a position sensitive neutron detector which consists of a long cylindric liquid scintillation tube,100 cm in length, 5.3 cm in inner diameter and two photomultipliers at the ends of the tube. The position information of the incident neutron is extracted from the time difference between the signals of the two photomultipliers. The measurements were carried out on the Cockcroft–Walton accelerator with rotational target at Tsinghua University. The angle between the associated $\alpha$ particle detector and the deuteron beam is 17°(as near as possible to 180°) to reduce the kinematic shifts of associated neutron beam with the T–Ti target ageing. The experimental data are corrected for the multiple neutron scattering and flux attenuation effects in the samples by Monte Carlo method. The results are shown in Tables 1～3, where $\theta$ is the scattering angle, $\sigma$ is the differential cross section.

**Table 1 Differential elastic cross section for 14.8 MeV neutrons from Fe**

| $\theta$(degree) | 2.5 | 4.0 | 6.0 | 8.0 | 10.0 | 12.0 | 14.0 | 16.0 |
|---|---|---|---|---|---|---|---|---|
| $\sigma$(b / sr) | 3.15 | 3.04 | 2.55 | 2.25 | 2.27 | 2.01 | 1.54 | 1.24 |
| Error(%) | 4.0 | 5.3 | 4.0 | 3.5 | 3.7 | 6.2 | 6.9 | 7.5 |

**Table 2 Differential elastic cross section for 14.8 MeV neutrons from Cr**

| $\theta$(degree) | 2.5 | 4.0 | 6.0 | 8.0 | 10.0 | 12.0 | 14.0 | 16.0 |
|---|---|---|---|---|---|---|---|---|
| $\sigma$(b / sr) | 2.74 | 2.64 | 2.87 | 2.67 | 2.63 | 2.07 | 2.14 | 1.37 |
| Error(%) | 8.5 | 4.0 | 6.3 | 6.0 | 6.1 | 7.4 | 6.9 | 8.5 |

**Table 3 Differential elastic cross section for 14.8 MeV neutrons from Ni**

| $\theta$(degree) | 2.5 | 4.0 | 6.0 | 8.0 | 10.0 | 12.0 | 14.0 | 16.0 |
|---|---|---|---|---|---|---|---|---|
| $\sigma$(b / sr) | 3.27 | 3.13 | 2.87 | 2.67 | 2.63 | 2.07 | 2.14 | 1.26 |
| Error(%) | 6.0 | 6.5 | 6.3 | 6.0 | 6.1 | 7.4 | 6.5 | 8.5 |

## REFERENCES


[1] Qi Huiquan et al., INDC(CPR)–005 / G, INDC(CPR)–006 / L.

[2] Qi Huiquan et al., Proc. of the Inter. Conf. on Nuclear Data for Basic and Appl. Sci. Santa Fe, USA, 13–17 May, 1985, 2, p.1355.

[3] Qi Huiquan et al., Proc. of the Inter. Conf. on Nuclear Data for Sci. and Tec. MITO, Japan, May 1988, p. 799.

[4] Qi Huiquan et al., Communication of Nuclear Data Progress, 1989,12(1).

# II THEORETICAL CALCULATION

## SUMMARY REPORT OF RESEARCH WORKS CONCERNING FISSION PHYSICS AND NUCLEAR DATA IN THEORETICAL GROUP

Hu Jimin

(INSTITUTE OF HEAVY ION PHYSICS, PEKING UNIVERSITY)

### INTRODUCTION

Theoretical works of the nuclear data group in our institute are divided into two related topics : physics of fission and macroscopic model of nuclear structure. The progress of the research works in 1989 will be described as follows.

### 1 PHYSICS OF FISSION

Our main interest in fission physics is the study of fission mechanism and the estimation of fission fragment mass distribution. It has long been proposed that the fission of a nucleus with moderately high excitation can be considered as a diffusion process in the phase space of collective motion, that is, a Brownian motion. Simple model has been proposed to calculate fission probabilities with this model. So far, no realistic calculation of fission as a multi–dimensional Brownian motion was published. A preliminary attempt in this direction has been performed by us. The fission of $^{213}$Ac formed in the reaction $^{209}$Bi($\alpha$,f) was studied as a two dimensional Brownian motion. The two collective degrees of freedom were chosen as nuclear elongation and asymmetry, with potential energy surface calculated from the finite range model and the mass and dissipation parameters calculated from Werner Wheeler's model and the one body dissipation model. The resulting Langevin Equations were solved by Monte Carlo simulation of the random forces. Results of the calculations

were comparable with empirical results, with mass distribution broader than empirical data. A summary of this work was presented to the International Conference on Fifty Years with Nuclear Fission[1].

For low excitation and spontaneous fission, a detailed model calculations is still unfeasible. A more or less qualitative model may be applied to obtain a semi-empirical estimation of the post scission characteristics of such fission process. An empirical formula for primary fragment mass distribution was proposed with results in reasonable agreement with experimental data. Theoretical analysis of the potential energy surface with two center shell model was carried out in support this model[2~4].

## 2 MACROSCOPIC MODEL OF NUCLEAR STRUCTURE

For a realistic study of the fission process, it is necessary to have a nuclear model valid for nucleus with large deformation and charge redistribution. With appropriate importance, the model developed by us may meet this requirement. In this year, we have calculated the charge distributions of deformed nuclei with results in good agreement with experimental findings[5]. To calculated nuclear masses, we have adopted the microscopic energy corrections given by Moller and Nix. In recent work, we have analyzed his correction. It is shown that the error involved in using their values is within the mean square root deviation of our calculation. It is also shown that there may be certain systematic deviations from empirical masses for light nuclei ($A < 100$). It is expected that an improvement of the microscopic energy correction may lead to better agreement of the calculated nuclear masses[6].

## REFERENCES


[1] Zhong Yingxiao, Hu Jimin, Fission as a Multi-Dimensional Brownian Motion, Inter. Conference on Fifty Years with Nuclear Fission, NAS, Washinton D. C. and NIST, Gaithersburg, Maryland, April 25-28, 1989.

[2] Wang Fucheng, Hu Jimin, A Semi-Empirical Formula on the Pre-Neutron-Emission Fragment Mass Distribution in Nuclear Fission, China Nucl. Sei. and Technology Report. CNIC-00183 PU-0001 (1988).

[3] Wang Fucheng, Hu Jimin, A Study of the Multimodel Fission Model, J. Phys. G: Nucl. & Part. Phys. 15(1989)829-848.

[4] Wang Fucheng, Hu Jimin, Transformation Between Pre - and Post-neutron emission Fragment mass distributions, CNIC - 00293 PU - 0002 (1989).

[5] Zheng Chunkai, Charge Density Distributions of Deformed Nuclei, to be published in the Proc. 50th Anniversary of Nuclear Fission Conference (1989).

[6] Hu Jimin, Zheng Chunkai, Xu Furong, Microscopic Correction of the Macroscopic Model, to be published in High Energy & Nuclear Physics.

# CALCULATIONS OF NEUTRON ELASTIC AND INELASTIC SCATTERING FROM $^{7}$Li

Zhu Yaoyin Zhang Yujun Li Zhiwen

(JILIN UNIVERSITY, CHANGCHUN)

## ABSTRACT

The fast neutron elastic scattering from $^{7}$Li have been analysed by means of the optical model. It was found that it is necessary to decrease the real–well diffuseness slowly with increasing energy. The microscopic DWBA were used to calculate neutron inelastic scattering by $^{7}$Li to the excited states at 0.478 MeV and 4.6 MeV. In the DWBA calculation, some parameters have been chosen as energy dependent parameters in order to improve the computation.

## INTRODUCTION

It is necessary to compute the elastic and inelastic scattering of neutrons by $^{7}$Li. For example, neutron inelastic scattering by $^{7}$Li to the excited state at 0.47 MeV is very important, but there are few experimental data dealing with this subject [1]. When the incident energy is very high, to distinguish the inelastic neutron from elastic neutron is more difficult, therefore, to obtain the corresponding experimental data is more diffecult too.

The fast neutron elastic scattering from $^{7}$Li have been analysed by means of the optical model. The direct interaction theory and a microscopic DWBA were used to calculate neutron inelastic scattering by $^{7}$Li to the excited states at

0.47 MeV and 4.6 MeV.

## 1 THE OPTICAL MODEL ANALYSIS

The fast neutron elastic scattering from $^7$Li have been analysed by means of the optical model. The potential of Woods–Saxon form is used in the optical model potential,

$$V(r) = -Uf(r,r_1,a_1) + 14Wa_2\frac{\mathrm{d}}{\mathrm{d}r}f(r,r_2,a_2) + U_s(\frac{h}{m_\pi c})^2\frac{1}{r}\frac{\mathrm{d}}{\mathrm{d}r}f(r,r_3,a_3)\vec{\sigma}\vec{L}$$

$$f(r,r_j,a_j) = [1+\exp(\frac{r-r_jA^{\frac{1}{3}}}{a_j})]^{-1} \qquad (j=1,2,3)$$

where $U$, $W$ and $U_s$ are the depth parameters of the real–well, the imaginary potential and spin–orbit term respectively, $r_j$ are the radius parameters and $a_j$ are the surface–diffuseness parameters.

The first consideration of the optical model analysis is the choice of the parameters. For the medium mass and heavy nuclei, there are generally accepted optical potential parameters. The potential depth parameters usually are dependent on energy. Because the individualities of light nuclei are very intense, thus there are not common optical potential parameters. We consider that when the incident neutron energy is not very high, the elastic scattering cross section and the angular distribution are more sensitive to the surface action of the optical potential real–well than its interior action for the light nuclei. Thus they are sensitive to the real–well diffuseness. In this paper, we regard the real–well diffuseness $a_1$ as a linear function of incident energy.

P. W. Lisowski et al. had pointed out this idea and analysed the neutron scattering from $^3$He[2]. But in the past few years, this idea had not been noticed. We think that it ought to be emphasized.

For the total cross section of n+$^7$Li system, there is a broad maximum at energy region near $E_n$= 5 MeV (the incident neutron energy in laboratory frame). According to energy level scheme, $E_n$= 3.8, 4.6, 5.08 and 5.8 MeV correspond to the excited states of compound–system $^8$Li, which are 5.4 , 6.1, 6.53 and 7.1 MeV. These show that the compound nucleus effect is very important at energy region near $E_n$= 5 MeV. In the energy range 6.97~20 MeV, the change of the elastic and total cross section of n+$^7$Li reaction is slow. In order to avoid the influence of the compound elastic scattering, the optical model analysis of neutron scattering from $^7$Li is confined to 6.97~20 MeV energy range in the

present paper.

The experimental data of total cross section take from the Ref.[3]. For the elastic scattering at 7～14 MeV energy range, the experimental data take from the Ref.[1].

At first, we alone adjusted the parameters aiming at 8.96 and 13.94 MeV. We found that regarding the real-well diffuseness $a_1$. the imaginary-well depth $W$ and the spin-orbit term depth $U_s$ as a linear function of incident energy can obtain good agreement with the experimental data. Afterward, we jointly adjusted the parameters aiming at 6.97, 7.97, 8.96, 9.96, 10.95, 12.94 and 13.94 MeV. At last, we obtained a set of the optical potential parameters :

$U=39.17104$ MeV, $a_1=(0.80279\sim0.0238\text{Ec})$fm, $r_1=1.4715$ fm

$W=(-0.82084+0.64642\text{Ec})$ MeV, $a_2=0.3502$fm, $r_2=1.3988$ fm

$U_s=(9.51855-0.35882\text{Ec})$ MeV, $a_3=0.12076$fm, $r_3=1.3034$ fm

The comparison of the calculated results of total cross section with the experimental data has been given in Table 1. It has been given in the Fig. 1 to compare the elastic scattering angular distribution containing the inelastic scattering to the excited state at 0.478 MeV with the experimental data. As can be seen from Table 1, the deviation of the total cross section is less than 3%. The better agreement with experimental data has been obtained for the elastic scattering angular distribution, especially for $E_n>9$ MeV energy region. Since the effect of compound elastic scattering has not been considered, it is reasonable that our calculated results of elastic scattering are lower than experimental data when $E_n$ is less than 8 MeV.

**Table 1 the comparison of calculated and evaluated total cross sections**

| $E_n$(MeV) | 7 | 8 | 9 | 10 | 11 | 12 | 13 | 14 |
|---|---|---|---|---|---|---|---|---|
| $\sigma_T^{eva}$(mb) | 1964 | 1855 | 1764 | 1692 | 1628 | 1568 | 1512 | 1458 |
| $\sigma_T^{cal}$(mb) | 1924 | 1835 | 1763 | 1700 | 1642 | 1590 | 1542 | 1498 |

## 2 THE DISTORTED-WAVE BORN APPROXIMATION

When the direct interaction theory was used to calculate neutron inelastic scattering from $^7$Li, we had applied perturbation theory in the form of a microscopic DWBA. We regard the interaction as the sum of the constituent nucleon-nucleon interaction and use a finite-range interaction of the form

$$V=\sum_{i=1}^{A}V_{oi}$$

$$V_{0i} = -V_0[W + MP'_{0i} + BP^{\sigma}_{0i} - HP^{\tau}_{0i}]\exp(-\gamma r^2_{0i})$$

where $W$, $B$, $H$ and $M$ are the strength of Wigner, Bartlett, Heisenberg, and Majorana force, $\gamma$ is a parameter of Gaussian potential, $r_{0i}$ is the radial distance, $V_0$ is the depth of the potential well. The wave functions of shell model are used for the initial and final state function of $^7$Li. The all possible configurations of $1P$ shell have been considered and the state functions of $^7$Li are given in Table 2.

**Table 2 The state functions of $^7$Li**

| $T$ | $J^{\pi}$ | $E_x$ | $P^{13}$ | $P^{12}_{(12)}P$ | $P^1P^2_{(10)}$ | $P^{12}_{(02)}P$ | $P^{12}_{(01)}P$ | $P^{12}_{(10)}P$ | $P^1P^2_{(01)}$ | $P^3$ |
|---|---|---|---|---|---|---|---|---|---|---|
| $\frac{1}{2}$ | $\frac{3^-}{2}$ | 0 | 0.6843 | −0.3256 | −0.5548 | | −0.2926 | | −0.1799 | |
| $\frac{1}{2}$ | $\frac{1^-}{2}$ | 0.478 | 0.3117 | | | | 0.3147 | 0.767 | 0.0778 | −0.4569 |
| $\frac{1}{2}$ | $\frac{7^-}{2}$ | 4.63 | −0.6024 | | | 0.7982 | | | | |

where $E_x$ is excitation energy of $^7$Li, $P'$ or $P$ express the shell whose spin is $3/2$ or $1/2$, respectively. We treat the wave functions of the harmonic oscillator as the radial parts,

$$R_{nl}(r) = U_{nl}(r)/r$$

$$U_{nl} = \sqrt{2\nu^{l+\frac{3}{2}}(n-1)!\ /[\Gamma(n+l+1/2)]}\,\gamma^{l+1}\exp(-\nu r^2/2)L^{l+\frac{1}{2}}_{n-1}(\nu r^2)$$

After interaction potentials and wave functions chosen, we can deduce the calculation formulas of the integral and differential cross sections for neutron inelastic scattering[4].

When the program was composed, the corresponsive formulas were rewritten[5]. Then the adjustable parameters are $V_0$ , $\gamma$, $M$, $B$, $H$, and $\nu$.

In the past, we thought that above parameters were independent on

energy[4]. However, the distorted-wave functions were calculated by means of the optical model, and some optical potential parameters vary with the incident neutron energy linearly. Therefore, there is the contradiction on the theoretical grounds. The computations of the differential cross section disagree with the experimental data, too. Thinking the facts that the neutrons might more close to the target nucleus with increasing of the incident neutron energy and interaction might be stronger, we choose some parameters which vary with the incident neutron energy.

For neutron inelastic (0.478 MeV level) scattering by $^7$Li, all parameters are shown below,

$$V_0 = 68.54+0.912E_n, \qquad \gamma = 0.021+0.00674E_n,$$
$$M = 0.392, \quad B = 0.127, \quad H = 0.109, \quad \nu = 0.586 .$$

As illustrated in Fig. 1, the calculations of neutron inelastic (0.478 MeV level) scattering by $^7$Li have been improved. The integral cross sections accord with the results in ENDF / B-6. There are not the accurate experemental data of the angular distribution at present, we can not make an exact comparison between the calculational and experimental data.

The angular distribution of elastic scattering have been computed by means of the optical model, the DWBA were used to calculate the inelastic scattering to the excited state at 0.478 MeV (Fig. 1). Their sum is in agreement with the experimental data, therefore the calculations of the inelastic (0.478 MeV level) scattering are available. For neutron inelastic (4.63 MeV level) scattering by $^7$Li, because of a change of excitation energy the outgoing neutron energy will change. Therefore the effect of energy dependence of the optical potential parameters will be stronger. Then $V_{0i}$ is really the effective interaction, for the different excited state it may be adjusted. For the higher excited state the depth of the potential well $V_0$ should be bigger. After adjusting,

$$V_0 = 68.54+3.78E_n$$

other parameters do not change.

As illustrated in Fig. 2, the calculations of neutron inelastic (4.63 MeV level) scattering by $^7$Li are lower than the measured results of H. H. Hogue et al.[1]. The new measured values are the results of S. Chiba et al.[6]. When the parameters were adjusted, we adopted these experemental data.

The authors are grateful to Dr. Yu baosheng for his helpful discussions.

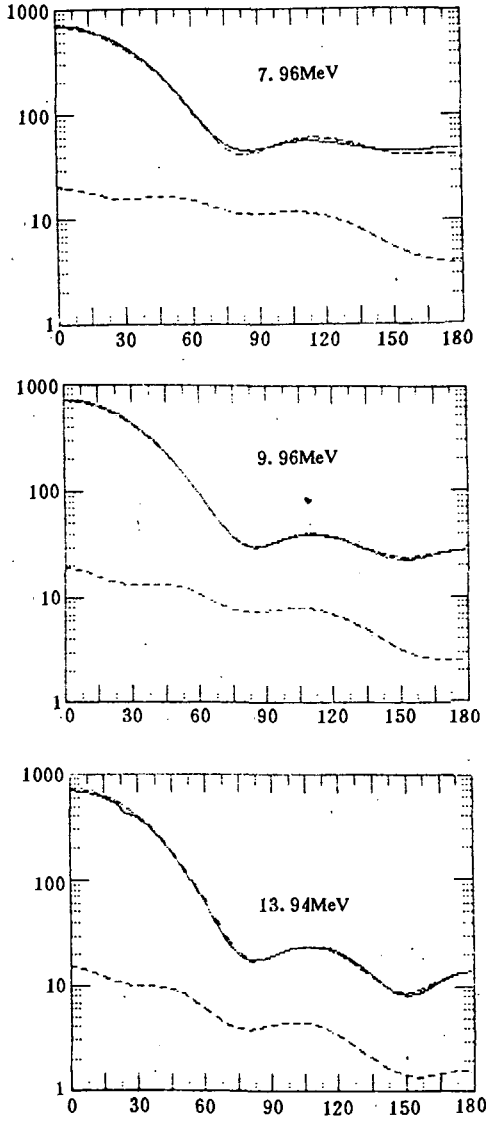


Fig. 1 Angular distributions of elastical and inelastically ($Q=-0.478$ MeV) scattering neutrons from $^{7}$Li

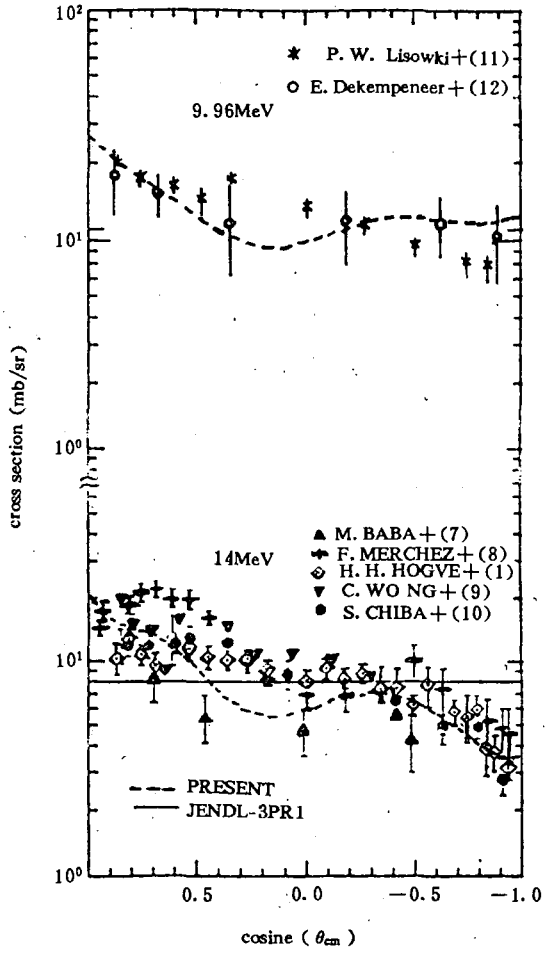


Fig. 2 Angular distributions of inelastical scattering neutrons from second level ($Q=-4.63$ MeV) of $^{7}$Li

## REFERENCES

[1] H. H. Hogue et al., Nucl. Sci. and Eng., 69, 22(1979).

[2] P. W. Lisowski et al., Pro. of the Inter. Conf. on the Interaction of Neutron with Nuclei, 2, 1444(1976).

[3] CNDC, hsj–79250(bp) 65 (1978).

[4] Zhu YaoYin et al., hsj–78217(11js).

[5] Zhu Yaoyin et al., Chin. J. of Computational Physics vol. 6, No. 4, 407(1989).

[6] S. Chiba et al., Nucl. Sci. and Tech., 25, 210(1988).

[7] M. BaBa et al., Proc. Int. Conf. on Nuclear Cross Sections for Technology, Knoxville, 1979, 43(1980).

[8] R. Merchez et al, Nuclrar Data for Reactors, Vol. 1, 393 (1967) and de Phys., colloque, 27, 1～61 (1966).

[9] C. Wong et al., Nucl. Phys., 33, 680 (1962).

[10] S. Chiba et al., J. Nucl. Sci. and Tech. 22, 771 (1985).

[11] P. W. Lisowski et al.,LA–8342(1980).

[12] E. Dekempeneer et al., Nucl. Sci. and Eng., 97, 353 (1987).


# PROGRESS ON THEORETICAL CALCULATION


Liu Jianfeng Zhang Xizhi Lu Zuhui

(DEPARTMENT OF PHYSICS, ZHENGZHOU UNIVERSITY)


## INTRODUCTION

Since 1989, on the basis of the calculation program NPPD–1[1] of Gamma–ray production data, the calculation program NPPD–2 of neutron reaction data in the energy region from $10^{-11}$ to 20 MeV has been researched with extending the energy from 5 to 20 MeV and the calculation function of emission particle energy spectra. The program will be presented to UNIFY program as a block of Gamma–ray production data.

So far, the program has been finished and the calculations for oxygen are being done in order to test the program. The ENDF / B–IV format is as the

output format, and the calculation function of isomeric state cross sections is going to be taken into account in this program.

## 1 THE PROGRAM NPPD–2

Fig. 1 shows the reaction channels in n+$^{40}$Ca which are taken into account in NPPD–2. Since more attention has been paid to the theoretical calculation of gamma–ray production data, different theoretical models and calculation formulas are used in different energy regions divided according to the (n,$\gamma$) reaction mechanisms.

In the thermal and resonance region, the cross sections of various reaction channels are calculated by using the resonance parameters. For (n,$\gamma$) reaction, besides the compound statistical process, the non–statistical effects which are considered in this region are potential capture[2], valence capture[3] and the interference effects between them. In the continuous region of the nuclear reactions, when the neutron incident energy is less than 5 MeV, the cross sections of various channels are calculated by using the Hauser–Feshbach's theory with the width fluctuation correction factor[4]. The transmission coefficients of particles are calculated by using the optical model. The non–statistical effects of the (n,$\gamma$) reaction are the capture in elastic channels [5] of the compound nucleus and the capture in inelastic channels of the compound nucleus[6]. When the incident neutron energy is higher than 5 MeV, the pre–equilibrium correction is used for the calculations of the reaction cross sections and the non–statistical effect of the (n,$\gamma$) reaction is the direct and semi–direct captures[7].

In this program, the cascade $\gamma$–de–excitations of the compound nucleus and residual nucleus are described by means of the Troubetzkoy's statistical model[8] and the conservation relations of angular momentum and parity are considered.

This program may be used for the calculations of the natural element with the number of isotopes less than 10 and the following data can be given :

1. Total cross section and the cross sections of every channels.
2. Gamma–ray multiplicity, gamma–ray production cross section and gamma–ray spectra.
3. The energy spectra of every particle channels.
4. Angular distribution of elastic and the separate inelastic channels.

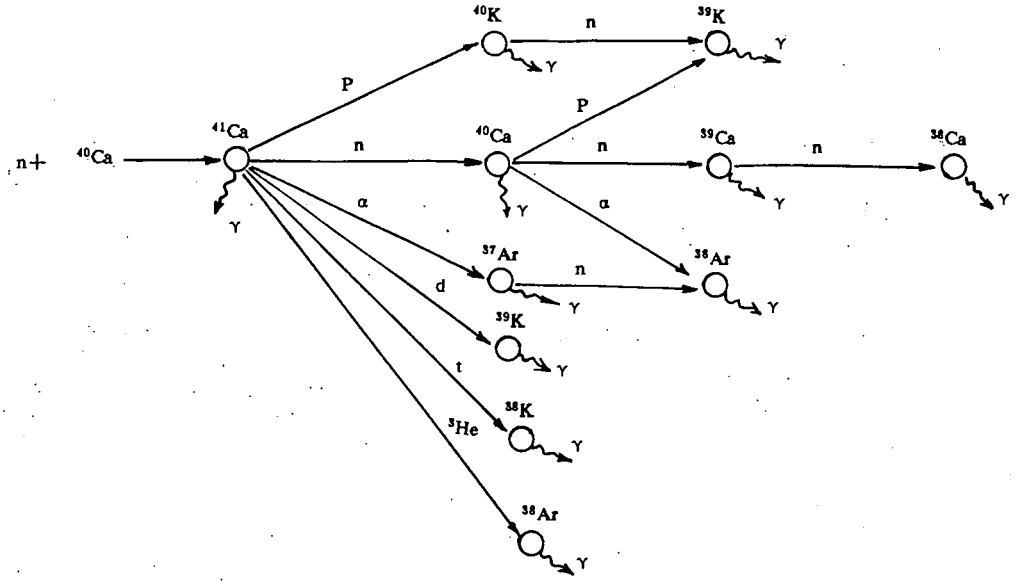


Fig. 1 The channels considered in NPPD–2

## REFERENCES


[1] Liu Jianfeng et al., CNDP, No. 1(1989)36.

[2] A. M. Lane, J. E. Lynn, Nucl. Phys., 11(1959)646.

[3] J. E. Lynn, The Theory of Neutron Resonance Reaction, (Clarendon Oxford, 1968).

[4] Su Zongdi, High Energy Physics and Nuclear Physics, 3(1979)80.

[5] Y. K. Ho and M. A. Lone, Nucl. Phys., A406(1983)1.

[6] Liu Jianfeng, High Energy Physics and Nuclear Physics, 3(1983)355.

[7] G. E. Brown, Nucl. Phys., 57(1964)339.

[8] E. S. Troubetzkoy, Phys. Rev., 122(1961)212.


# A R–MATRIX ANALYSIS FOR $^{17}O$ SYSTEM


Chen Zhenpeng Qi Huiquan

(DEPARTMENT OF PHYSICS, TSINGHUA UNIVERSITY)


The evaluation of n+ $^{16}O$ in neutron energies from 0 to 6.2 MeV with R–matrix theory was finished by a cooperation with Dr. Hale and Dr. Young of the LANL, USA. The code used was EDA of LANL, and our code RAC was used to check the calculation, both produced the same results. The final results were included in ENDF / B–VI and the CENDL of China. The old analysis was based on the ENDF / B–V evaluation, which dated to the mid 1970's. After that a lot of new experimental data were given out. The new analysis in-

cluded extensive new experimental data and level structure information at excitation energies below 10.5 MeV.

The new measurements of the n+ $^{16}$O total cross section by Larson[1], Cierjacs[2] were included at neutron energies from 1 keV to 6.5 MeV. We also included new measurements of elastic scattering differential cross section and polarization in an energy range of 2.0 to 4.0 MeV by Drigo[4].

The channel configuration and data summary for the analysis are given in Table 1. The R–matrix parameters involve 45 levels. About 110 none–zero R–matrix parameters including channel radii were varied simultanously to fit the more than 3500 data points, which included the three reactions considered. The obtained level structure agrees for the most part with the recommended data[5], but with different parity assignments for some of the resonances and minor differences in positions and widths for the others.

The obtained results agree with experimental data pretty well for all reactions. As an example, in Fig.1 all details of the considerable structures in total cross section and the ( n,α) cross section are well described.

**Table 1 Channel Configuration and Data Summary for the $^{17}$O System by R–Matrix Analysis**

| Channel | $L$(max) | Radii(fm) |
|---|---|---|
| n+$^{16}$O | 4 | 4.44 |
| α+$^{13}$C | 4 | 6.01 |

| Reaction | Energy Range(MeV) | Observable Types | Data Pornts |
|---|---|---|---|
| $^{16}$O(n,n)$^{16}$O | $E_n$=0~6.5 | Total, Dif., Polar. | 2421 |
| $^{16}$O(n,α)$^{13}$C | $E_n$=0~6.0 | Inte., Dif., Polar. | 904 |
| $^{13}$C(α,α)$^{13}$C | $E_n$=0~4.6 | Dif., | 207 |
| Total | | 7 | 3532 |

## REFERENCES


[1] D. C. Larson, ORELA Measurement to Meet fussion Energy Neutron Cross Section Needs, Proc. symp. on Neutron Cross Section from 10 to 50 MeV (BNL–NCS–51245), 277(1980).

[2] S. Cierjacks et al., J. Nucl. Inst. Meth., 169, 185(1980).

[3] J. K Bair F. X Hass, Phys. Rev., C7, 1356(1973).

[4] L. Drigo et al., Nuov. Cim., 31, 1(1976).

[5] F. Ajzenberg–Selove, Nucl. Phys., A460, 77(1986).

Fig. 1 Total (bottom) and reaction (top) cross sections for n+$^{16}$O at energies up to 6 MeV

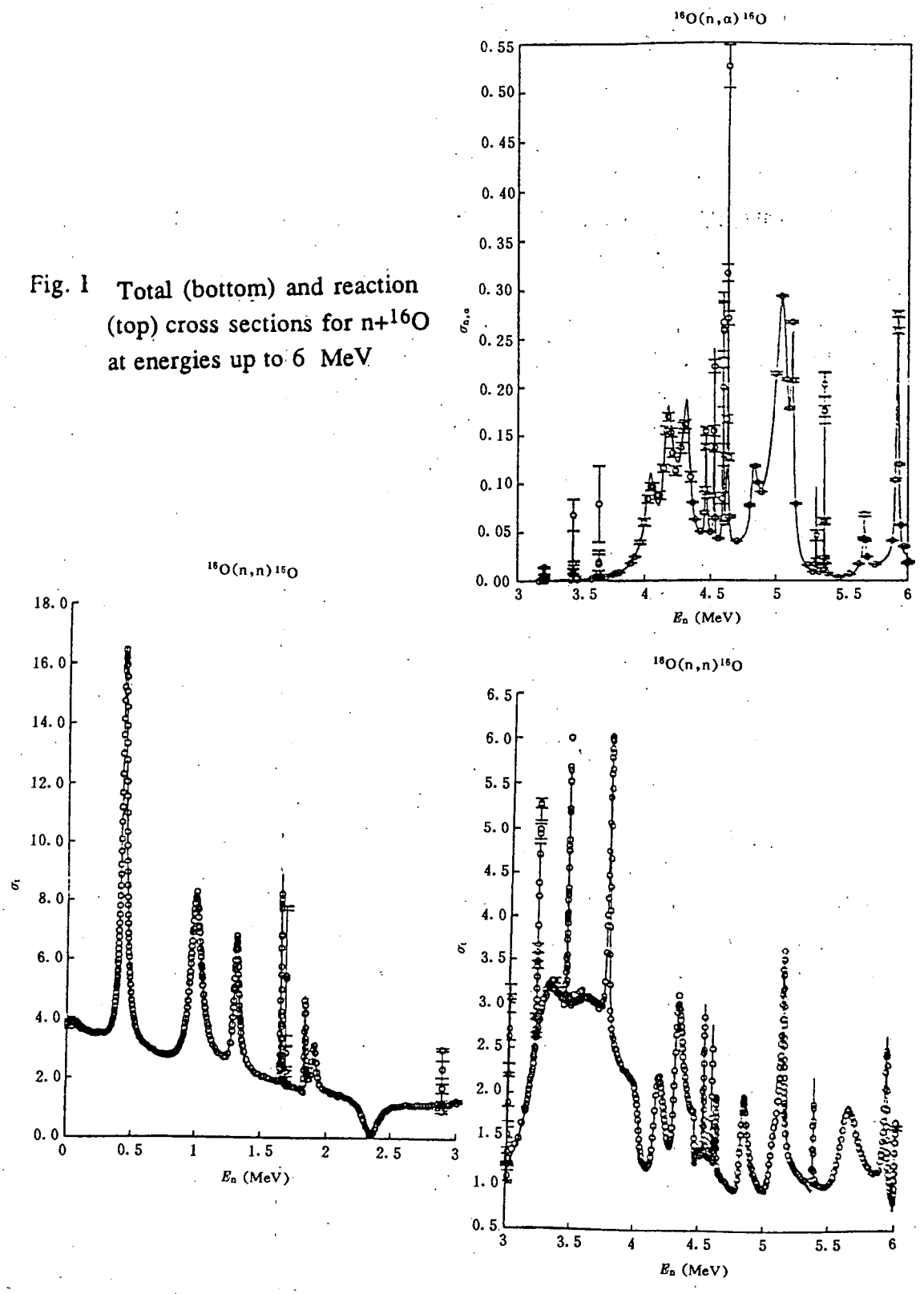

# PROGRESS IN CALCULATION OF FISSILE NUCLEI

Cai Chonghai

(DEPARTMENT OF PHYSICS, NANKAI UNIVERSITY)

Last year, we completed three computer programs for calculating fissile nuclei. They are FUP1[1] (a unified program for calculating all fast neutron data of fissile nuclei), ASFP[2] (a program for automatically searching for a group of optimal fission parameters) and ASOP (a program for automatically searching for an optimum set of the neutron optical model parameters for fissile nuclei). ASOP is similar to AUJP, only different in subroutine HF(ASOP contains fission reaction but AUJP contains reactions emitting charge particles).

Recentely, we use ASFP to adjust the fission parameters of the first and second plateaus of $^{238}$U and $^{237}$Np, of the third plateau of $^{238}$U and the first plateau of $^{236}$U in $E>$ 3 MeV energy region (by PE theory), and the parameters of $^{238}$U and $^{237}$Np in $E<$ 3 MeV (by HF theory). And then we calculate all neutron reaction cross sections of $^{238}$U in 0.02 ~ 20MeV energy region by using FUP1. In our calculation, the optical model parameters are taken from Q. B. Shen et al.[3], the optical potential parameters of $^{237}$Np are substituted with those of $^{239}$Pu. The calculated cross sections are quite well in agreement with experimental values except for $\sigma_{n,2n}$ and $\sigma_{n,3n}$ in 14 ~ 20 MeV energy region. The reasons of this disagreement are, we think, in ASFP and FUP1 we do not consider the direct (n,2n) reaction, and the Cameron formula of energy level density can not correctly express the discrete energy levels. The results of calculation and comparison with experimental values can be refered to Tang's paper[4]. The parameters of $^{238}$U needed in FUP1 calculation are as follows:

**Fission parameters in PE calculation ***

| | $V_f$ | $K_1$ | $K_2$ | $\Delta$ | $a$ | $\hbar\omega$ |
|---|---|---|---|---|---|---|
| $^{239}U$ | 5.535875 | 1.762433 | 0.040890 | 0.503345 | 29.644012 | 0.537708 |
| $^{238}U$ | 6.172938 | 2.171436 | 0.030130 | 0.902548 | 28.887817 | 0.795100 |
| $^{237}U$ | 6.031904 | 1.762614 | 0.202768 | 0.577677 | 29.526947 | 0.652000 |
| $^{236}U$ | | | | 1.160501 | 28.682846 | |

**Fission parameters in HF calculation ***

| EPSD = $\varepsilon-\Delta$ | $V_f$ | $K_1$ | $K_2$ | $\Delta$ | $a$ | $\hbar\omega$ |
|---|---|---|---|---|---|---|
| 1.251335 | 6.184927 | 3.296467 | 0.207348 | 0.503345 | 29.644012 | 0.537708 |
| | | | | 0.902548 | 28.887817 | |

The first row is for $^{239}U$, the second for $^{238}U$.

**Giant resonance parameters for ( n,$\gamma$) reaction**

| $S_{a01}$ | $S_{a02}$ | $G_{m1}$ | $G_{m2}$ | $E_{g1}$ | $E_{g2}$ |
|---|---|---|---|---|---|
| 0.30 | 0.35 | 1.77 | 4.55 | 10.58 | 13.87 |

The adjustable parameter $K$ in matrix element of exciton state transitionis taken as 400.0.

* The meaning of all above parameters can be refered to references [1] and [2].

## REFERENCES


[1] C. H. Cai et al., CNDP 3, 29(1990).

[2] C. H. Cai, ASFP, CNDP 3, 26(1990).

[3] Q. B. Shen et al., The Optical Model Calculation of Fissile Isotopes of U and Pu elements in the energy region from 1 keV to 20 MeV, Symposium on Nuclear Reaction Theory and its Application, Published by Atomic Energy Press, 1980, Beijing, p202.

[4] G. Y. Tang, CNDP 3, 35(1990).

# R–MATRIX ANALYSIS CODE (RAC)

Chen Zhenpeng Qi Huiquan

(DEPARTMENT OF PHYSICS, TSINGHUA UNIVERSITY)

A comprehensive R–matrix analysis code has been developed. It is based on the multichannel and multilevel R–matrix theory[1] and runs in VAX computer with FORTRAN–77.

This code is an automatically fitting one. All the R–matrix parameters are adjustable,which include channel radii, boundary condition numbers, positions and reduced width amplitudes of all energy levels considered.

With the code many kinds of experimental data for one nuclear system can be fitted simultanously. Those data may have different reaction channel. Usually they include total cross section, elastic scattering cross section, reaction cross section and polarization.

A new technology for developing code named The Optimize Method for Design Optimization Code[2] was used. So the CPU time can be reduced significantly.

We have made detailed comparison between our code RAC and code EDA of LANL[3]. With one set of R–matrix parameters, both codes produced the same calculation results ( Table 1 and Table 2 ).

The authors wish to thank Liu Manfen et al. of Jilin University for their generous help to us.

**Table 1 The differential cross section of $^{10}B(n,\alpha)^{7}Li^{*}$ for $E_n = 0.4$ MeV**

| Angle (degree) | RAC (China)(mb / sr.) | EDA(USA)(mb / sr.) |
|---|---|---|
| 0.00 | 14.624 | 14.621 |
| 20.00 | 14.161 | 14.160 |
| 40.00 | 12.841 | 12.840 |
| 60.00 | 10.950 | 10.951 |
| 80.00 | 8.759 | 8.757 |
| 100.00 | 6.607 | 6.606 |
| 120.00 | 4.753 | 4.753 |
| 140.00 | 3.363 | 3.362 |
| 160.00 | 2.154 | 2.513 |
| 180.00 | 2.230 | 2.230 |

**Table 2 The polarization of $^{16}O(n,n)^{16}O$ for $E_n = 2.56$ MeV**

| Angle (degree) | RAC (China) | EDA(USA) |
|---|---|---|
| 26.55 | 0.2771 | 0.2764 |
| 47.50 | 3.3694 | 0.3694 |
| 68.20 | 0.3468 | 0.3472 |
| 93.60 | 0.2356 | 0.2355 |
| 118.20 | 0.0332 | 0.0332 |
| 137.50 | −0.1125 | −0.1126 |
| 156.50 | −0.1083 | −0.1073 |

## REFERENCES


[1] A. M. Lane et al., Rev. Mod. Phys. 30, 257(1958).

[2] Z. P. Chen, Qi Huiquan, J. of Tsinghua University, IV, 1984.

[3] D. C. Dodder et al., EDA, An Energy Dependence Analysis Code for Nuclear Reaction, Unpublished.

# PRELIMINARY STUDY OF NEUTRON OPTICAL POTENTIAL PARAMETERS FOR FISSION PRODUCTS

## $A=90\sim140$, $E_n=0.1\sim20$ MeV

Li Shiqing Liu Yanping Zheng Kangxun

(WUHAN UNIVERSITY)

## ABSTRACT

Using the optimized optical potential parameters of 7 fission product nuclei (FP), a set of expirical optical potential parameters (EOP) for fission products ($A=90\sim140$, $E_n=0.1\sim20$ MeV) was obtained. The optical model calculations have been made for 12 FP using EOP and the results are better than that calculated results by using the BGP (optical model parameters of Becchetti and Greenlees) or MOP (microscopic optical).

## INTRODUCTION

The optical model is an important tool in nuclear data calculations that are used for reproducing experimental data and supplying nuclear data for some applications. Using experimental neutron data, we have adjusted the optimized optical parameters (OOP) of 7 fission products ($^{92}$Zr, $^{93}$Nb, $^{98}$Mo, $^{100}$Mo, $^{107}$Ag, $^{115}$In and $^{138}$Ba) respectively,and analyzed the dependence of OOP with the neutron energy $E$ and mass number $A$ of nucleus. Finally, a set of empirical optical potential parameters (EOP) for fission products (FP) is obtained. The purpose of this work is to use EOP to finish the optical model calculations for FP ($A=90\sim140$, $E_n=0.1\sim20$ MeV) which are lack of experimental data.

The optical potential is as follows:

$$V(r)=V_C(r)+V_R(r)+iV_I(r)+2V_{SO}(r)(S\cdot L) \qquad (1)$$

where

$V_c(r)$ is Coulomb potential,

$$V_R(r) = -Vf(r, r_1, a_1),$$
$$V_I(r) = 4w_s a_2 \, \mathrm{d}/\mathrm{d}r f(r, r_2, a_2) - Uf(r, r_3, a_3), \quad (2)$$
$$V_{SO}(r) = (V_{SO}/r)\mathrm{d}/\mathrm{d}r f(r, r_4, a_4);$$

and $f(r, r_i, a_i) = \{1+\exp[(r-r_i A^{1/3})/a_i]\}^{-1}$, $i = 1, 2, 3, 4.$

The energy dependences of $V$, $U$ and $W_s$ written as:

$$V = V_0 + V_1 E + V_2 E^2 + V_3(N-Z)/A + V_4 Z/A^{1/3},$$
$$U = U_0 + U_1 E, \quad (3)$$
$$W_s = W_0 + W_1 E + W_2(N-Z)/A.$$

The first consideration of the optical model analysis is the choice of the parameters. Among 22 parameters, $V_0$, $W_0$, $U_0$, $r_1$, $r_2$, $a_1$, $a_2$ are more sensitive in cross section calculations according to Refs. [1～3].

Let $a_4 = a_1$, $a_3 = a_2$, $r_4 = r_1$, $r_3 = r_2$, and take $R_c$, $V_1$, $V_2$, $V_3$, $V_4$, $W_2$, $V_{SRO}$ as constants. Because the energy dependence, pairing and Coulomb corrections are considered in eq. (3), the sensitive parameters $V_0$, $W_0$, $U_0$, $r_1$, $r_2$, $a_1$ and $a_2$ are expanded with $A$ and $A^{1/3}$ and fitted the experimental data.

## 1 EMPIRICAL OPTICAL POTENTIAL PARAMETERS (EOP)

The obtained empirical parameters (EOP) are as follows:

$$V_0 = 51.9265 - 0.0175A - 1.3004 \times 10^{-5}A^2 - 7.5132 \times 10^{-7}A^3,$$
$$W_0 = 12.0829 - 0.006601A^{2/3} - 1.0367 \times 10^{-4}A^{4/3},$$
$$U_0 = 1.3542 - 0.001487A + 2.215 \times 10^{-5}A^2,$$
$$r_1 = 1.1094 + 0.001089A + 2.2029 \times 10^{-6}A^2,$$
$$r_2 = 1.2417 + 0.001187A + 5.5634 \times 10^{-6}A^2,$$
$$a_1 = 0.9099 - 0.002182A - 3.3397 \times 10^{-6}A^2,$$
$$a_2 = 0.6032 - 0.001420A - 7.9565 \times 10^{-7}A^2;$$

and take

$$V_1 = -0.33066,$$
$$V_2 = 0.003703,$$
$$W_1 = -0.088,$$
$$U_1 = 0.11052.$$

## 2 THE RESULTS AND ANALYSIS

The neutron data of twelve fission products ($A = 90 \sim 140$, $E_n = 0.1 \sim 20$ MeV) have been calculated by using EOP, and the results are listed in Table 1. The values calculated are compared with the experimental data. In the same

way as in Ref. [4], the objective function $\chi^2$ is used to demonstrate the degree of agreement of the calculated values with experimental data (see Table 1). The calculations using the microscopic optical potential (MOP)[5] and phenomenological optical–model parameters (BGP) by Becchetti and Greenlees[6] are also given in Table 1. The results show that the EOP parameter is better than MOP or BGP in the calculations of neutron data of FP. Therefore, EOP is available and reliable in calculations of neutron data of FP ($A=90\sim140$, $E_n=0.1\sim20$ MeV) when no or not enough experimental data can be used. It is also useful for optical model calculation to choose EOP as an initial parameter, in this case the CPU time can be saved a lot.

**Table 1 Comparison between calculated and experimental values**

| NUCLEAR | PARAMETER | $\chi^2_{\sigma_t}$ | $\chi^2_{\sigma_{non}}$ | $\chi^2_{\sigma_{el(\theta)}}$ | $\chi^2$ |
|---|---|---|---|---|---|
| $^{138}$Ba | BGP | 32.1123 | 4.9461 | 34.7927 | 22.2601 |
| $^{138}$Ba | MOP | 23.7640 | 2.1720 | 32.8244 | 16.7993 |
| $^{138}$Ba | EOP | 3.7516 | 1.1743 | 5.3995 | 2.9911 |
| $^{100}$Mo | BGP | 1.6470 | 3.5527 | 2.0865 | 2.0379 |
| $^{100}$Mo | MOP | 0.2381 | 3.1505 | 2.4848 | 2.2213 |
| $^{100}$Mo | EOP | 1.5021 | 0.1939 | 1.8574 | 1.3433 |
| $^{92}$Zr | BGP | 4.1404 | 0.9340 | 23.1792 | 9.0887 |
| $^{92}$Zr | MOP | 9.5594 | 19.1045 | 18.2161 | 14.8869 |
| $^{92}$Zr | EOP | 2.3779 | 2.5673 | 8.2871 | 3.3032 |
| $^{98}$Mo | BGP | 1.7847 | 10.5119 | 10.3969 | 6.1339 |
| $^{98}$Mo | MOP | 3.2187 | 1.6907 | 5.6627 | 2.9512 |
| $^{98}$Mo | EOP | 1.6190 | 1.7387 | 4.1660 | 1.9823 |
| $^{107}$Ag | BGP | 1.7445 | 19.4681 | 18.7373 | 10.5199 |
| $^{107}$Ag | MOP | 4.2571 | 8.2431 | 18.0888 | 7.4808 |
| $^{107}$Ag | EOP | 0.5622 | 6.6443 | 10.2074 | 4.0486 |
| $^{141}$Pr | BGP | 9.4672 | 70.0115 | 34.0210 | 35.2416 |
| $^{141}$Pr | MOP | 2.2971 | 2.1088 | 13.4526 | 3.6205 |
| $^{141}$Pr | EOP | 1.0073 | 16.9224 | 15.5290 | 8.7907 |
| $^{90}$Zr | BGP | 1.1909 | 10.6239 | 6.9041 | 5.4424 |
| $^{90}$Zr | MOP | 5.9013 | 11.7370 | 12.7890 | 8.9509 |
| $^{90}$Zr | EOP | 1.5317 | 11.9241 | 8.6464 | 6.3432 |
| $^{92}$Mo | BGP | 1.2327 | 11.1024 | 8.2639 | 5.8127 |
| $^{92}$Mo | MOP | 3.8547 | 3.6789 | 7.8840 | 4.2925 |
| $^{92}$Mo | EOP | 0.3869 | 4.1609 | 2.3264 | 2.0446 |
| $^{133}$Cs | BGP | 0.8353 | 13.2286 | 22.3384 | 8.1707 |
| $^{133}$Cs | MOP | 1.7047 | 13.6704 | 9.7453 | 7.1968 |
| $^{133}$Cs | EOP | 0.5305 | 2.6887 | 10.4105 | 2.5747 |

| | | | | | |
|---|---|---|---|---|---|
| $^{94}$Mo | BGP | 0.5938 | 7.5033 | 21.1984 | 5.7600 |
| $^{94}$Mo | MOP | 3.0143 | 1.9852 | 17.2272 | 4.4050 |
| $^{94}$Mo | EOP | 0.5520 | 0.8757 | 12.9480 | 2.2228 |
| $^{103}$Rh | BGP | 1.2204 | 14.5195 | 26.6099 | 9.3813 |
| $^{103}$Rh | MOP | 2.1707 | 2.7867 | 75.8544 | 11.6195 |
| $^{103}$Rh | EOP | 0.7607 | 2.7852 | 51.0283 | 7.8034 |
| $^{96}$Mo | BGP | 0.6108 | 6.1937 | 20.7606 | 5.2231 |
| $^{96}$Mo | MOP | 2.5260 | 2.6748 | 15.7712 | 4.2375 |
| $^{96}$Mo | EOP | 0.4673 | 0.7787 | 12.7433 | 2.1185 |

## REFERENCES


[1] J. Rapaport, Physics Reports, 87 (1982), 25.

[2] Zongdi Su, INDC(CPR)–013 / LI, INT(88)–1.

[3] E. D. Arthur, Nuclear Science and Engineering, 76 (1980) 137.

[4] Liu Yanping, Li Shiqing, Xiong Yuansheng, Communication of Nuclear Data Progress No.2, (1989), 69.

[5] a) Shen Qingbiao et al., Z. Physik, A 303 (1981), 69.

b) Shen Qingbiao et al., Nuclear Data for Science and Technology, Proc. Int. Conf. Antwerp, 6–10 Sept, 1982, p565.

c) Tian Ye et al, Chinese Journal of Nuclear Physics, Vol. 7, No. 2 (1985) 154 and Vol. 8, No. 1 (1986) 28.

[6] F. D. Becchetti and G. W. Greenlees, Phys. Rev., 182 (1969), 1190.


# A CALCULATION ON n–D SCATTERING CROSS SECTIONS IN THE ENERGY RANGE 0~20 MeV


Chen Jianxin Wang Yansen Qiu Zhihong
Yuan Zhushu Chen Chiqing

(DEPARTMENT OF NUCLEAR SCIENCE, FUDAN UNIVERSITY)

A calculation on n–D scattering cross sections with phase shift analysis[1] is carried out in the neutron energy range of 0～20 MeV. The dependences of the phase shifts $\delta_{lj}$ on the neutron energy are given by the effective range approximation with 4 partial waves for the energy region of 0～12 MeV,

$$k^{2l+1}\,\mathrm{ctg}\delta_{lj} = a_{lj} + 0.5 r_{lj} k^2 + p_{lj} k^4 \tag{1}$$

where $k$ is wave vector, $\delta_{lj}$, $r_{lj}$ the phase shift and decay factors, $l$ is orbital angular momentum. $a_{lj}$, and $p_{lj}$ are the adjustable parameters, in which the scattering lengths $(a_{02})^{-1}$ and $(a_{04})^{-1}$ are well known[2].

The dependences of the inelasticity factors $Y_{lj}$ on the neutron energies are given by the following formula :

$$Y_{lj} = \left\{1 + [(E_n - 3.339)(b_{lj} + g_{lj} E_n + f_{lj} E_n^2)]^2\right\}^{-1} \tag{2}$$

where $b_{lj}$, $g_{lj}$ and $f_{lj}$ are also the adjustable parameters. This formula is more reasonable than that given in Ref. [3], in which some values of $Y_{lj}$ are negative.

For the energy region of 11～20 MeV, the dependences of $\delta_{lj}$ and $Y_{lj}$ on the neutron energies are as follows :

$$\delta_{lj} = A_{lj} + B_{lj} E_n + C_{lj} E_n^2 + D_{lj} E_n^4 \tag{3}$$

$$Y_{lj} = F_{lj} + G_{lj} E_n + H_{lj} E_n^2 + J_{lj} E_n^4 \tag{4}$$

where $A,B,C,D,F,G,H$ and $J$ are adjustable parameters. Also the 4 partial waves are adopted. Based on the assumption of the charge symmetry in mirror scattering, the initial values of these parameters can be obtained very well by fitting the p–D phase shifts which have been given in Ref. [4].

An optimum set of parameters are obtained by fitting the experimental data which include total, (n,2n) and differential cross sections of n–D scattering[5] (see Tab. 1 and Tab. 2). It should be pointed that in the region of 11～12 MeV the weighted mean of the two methods are taken in order to get the smooth connecting and the better fit to the experimental data.

Comparing with the other work[3,6] and our earlier work[1], the calculated results have following features :

(1) The total calculated cross sections can reflect the inflection point from

the recent experimental data near 0.4 MeV, which can not be obtained by using the phase shifts given in Refs. [3] and [6] (see Fig.1).

(2) The errors of the calculated values for the total and (n,2n) cross sections are almost all smaller than that of the experimental data in the neutron energy region 0～20 MeV. Only for the few points of the total cross section, the errors are a bit larger than the experimental ones, but the relative errors are smaller than 1% (see Fig.2).

(3) The obtained differential elastic cross sections are in good agreement with the experimental values (see Figs. 3a～3d).

**Table 1 The phase shifts parameters * ($0<E_n<12.0$ MeV)**

| $^{\lambda}l$ | a | r | p | b | g | f |
|---|---|---|---|---|---|---|
| $^2S$ | −1.538+0 | 7.146+1 | −5.412+3 | −5.409−2 | 4.254−3 | 4.213−5 |
| $^2P$ | 8.930−1 | −2.412+2 | 1.074+3 | 4.927−2 | 4.678−3 | −3.454−4 |
| $^2D$ | 5.125−4 | 6.128−3 | 9.903−1 | −3.676−2 | 1.075−2 | −4.688−4 |
| $^2F$ | 1.110+3 | −7.442−2 | 8.614−2 | −1.120−1 | 7.423−3 | −2.520−5 |
| $^4S$ | −1.577−1 | 2.368+0 | −6.360−1 | 5.608−2 | −1.432−2 | 5.965−4 |
| $^4P$ | 5.951−3 | 5.698−1 | 1.697+0 | −5.517−3 | −4.967−4 | 3.727−5 |
| $^4D$ | −5.001−3 | 7.006−1 | −9.948+0 | −2.590−2 | 5.956−3 | −4.912−4 |
| $^4F$ | 1.231−1 | −1.247+0 | −9.481+0 | −2.367−2 | 4.446−4 | 1.801−5 |

* Dimension : $[a]=(\mathrm{fm})^{-(2l+1)}$, $[r]=(\mathrm{fm})^{-(2l-1)}$, $[p]=(\mathrm{fm})^{-(2l-3)}$, $[g]=(\mathrm{MeV})^{-1}$, $[f]=(\mathrm{MeV})^{-2}$.

**Table 2 The parameters * of the phase shifts curve (11.0 MeV$<E_n<$20.0 MeV)**

| $^{2s}l$ | A | B | C | D | F | G | H | J |
|---|---|---|---|---|---|---|---|---|
| $^2$S | 2.8130+0 | −7.2776−2 | 3.0615−4 | 4.1397−7 | 1.0961+0 | −6.3329−2 | 1.4993−3 | −7.3037−8 |
| $^2$P | −9.9973−1 | 1.8075−1 | −7.2908−3 | 4.2317−6 | 1.3480+0 | −9.6076−2 | 3.8446−3 | −1.7400−6 |
| $^2$D | −9.0000−2 | 1.7862−2 | −4.1584−4 | 2.7000−7 | 1.1150+0 | −1.6140−2 | 4.0100−4 | −1.5850−7 |
| $^2$F | −2.4604−2 | −6.8549−3 | 4.6010−4 | −7.5000−7 | 1.0129+0 | −1.4000−3 | −3.1000−5 | 1.7000−7 |
| $^4$S | 1.7588+0 | −3.9368−2 | 4.6285−4 | −1.6650−8 | 1.0942+0 | −1.5098−2 | 5.0628−4 | −2.1799−7 |
| $^4$P | 4.4672−1 | 1.9767−2 | −7.1241−4 | −3.4704−8 | 1.5118+0 | −8.7059−2 | 3.1988−3 | −1.3318−6 |
| $^4$D | −1.0725−1 | −7.5823−3 | 1.2925−4 | 1.8693−7 | 7.5632−1 | 5.1745−2 | −3.0590−3 | 2.1159−6 |
| $^4$F | 6.8000−2 | −3.6792−3 | 1.6117−4 | −8.9414−8 | 1.0015+0 | 4.3387−4 | −5.4343−5 | 1.8469−8 |

* Dimension : $[B]=[G]=(MeV)^{-1}$, $[C]=[H]=(MeV)^{-2}$, $[D]=[J]=(MeV)^{-4}$.

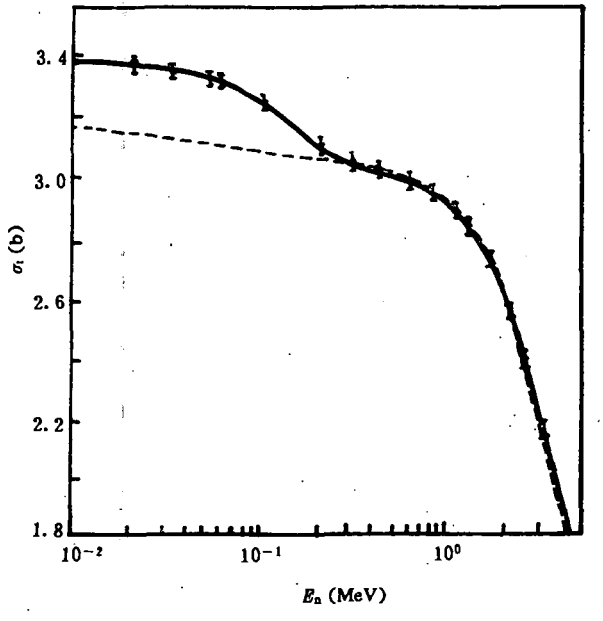


Fig. 1 The total cross sections for n−D interaction

—— this work

--- calculation from [6]

⊕ experimental data from [5]

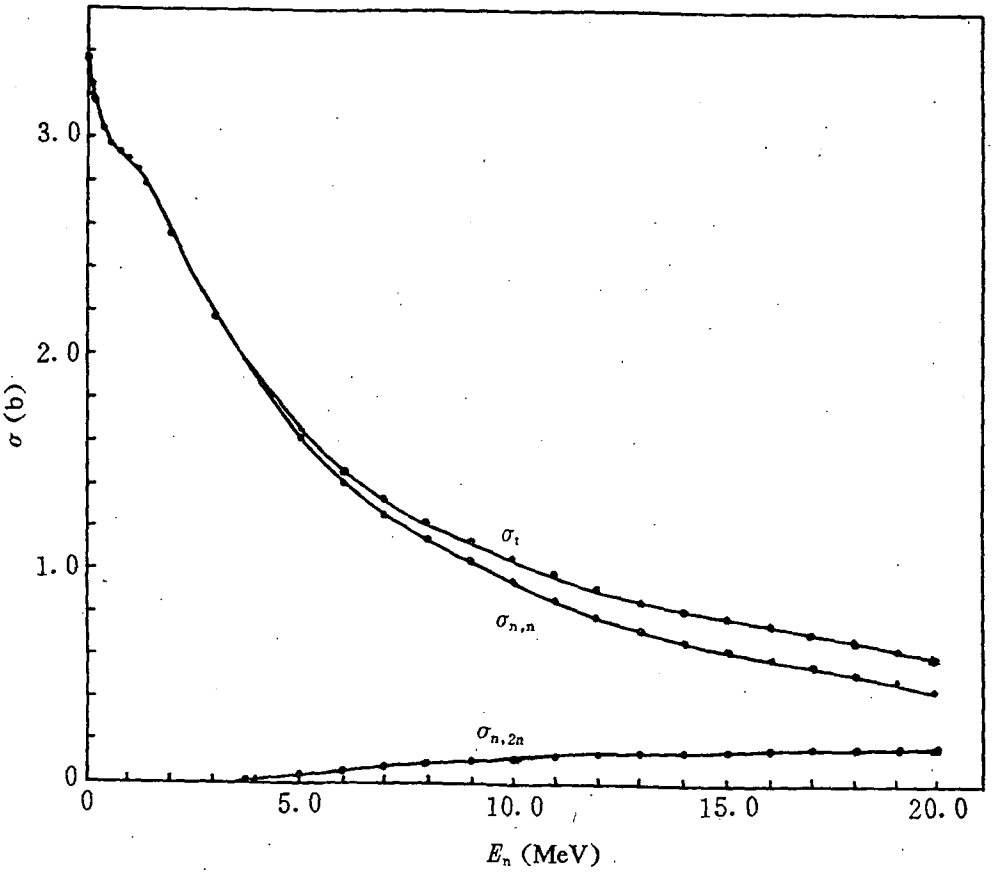


Fig. 2 The comparison of the calculated results with the experimental data for total, (n,n) and (n,2n) cross sections

— this work

• experimental data from [5]

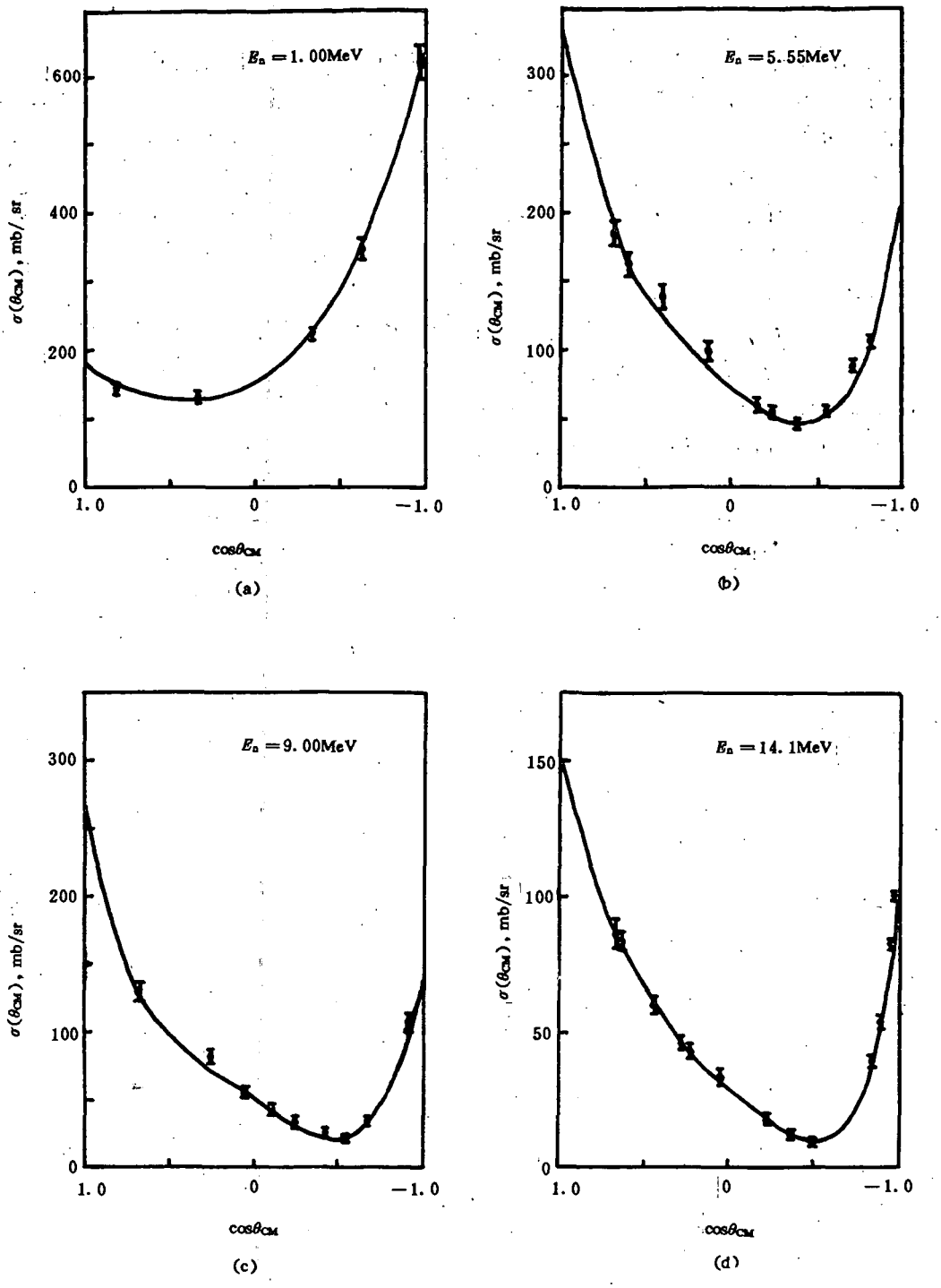


Fig. 3a～3d. The differential elastic cross sections for n–D scattering at some neutron energies

— this work

Φ experimental data from [5]

## REFERENCES


[1] Qiu Zhihong, Wang Yansen, Shen Xichu and Chen Jianxin, Theoretical Methods of Nuclear Reactions and Its Applications p18, Atomic Energy Publishing House, China(1980).

[2] D. R. Tilley et al., Nucl. Phys., A474, 1(1987).

[3] Carla Abulaffio & Asher Peres, NBS–425 Vol. II, Nuclear Cross Section and Technology (1975).

[4] J. Arvieux, Nucl. Phys., A221, 253(1974).

[5] Zhou Enchen, hsj–77075(bp) (1978); Huang Shengnian, hsj–77095(bp) (1978); Tang Hongqing, hsj–77171(bp) (1981); Cai Dunjiu, CNDP, 4 (1990); Zhuang Youxiang, Evaluation of Deuteron Neutron Data for CENDL–2(1990).

[6] R. Viennet, Nucl. Phys., A189, 431(1972).

# III DATA EVALUATION

## THE EVLAUATION OF $^{23}Na(n,\gamma)^{24}Na$ REACTION CROSS SECTION

Yuan Hanrong

(INSTITUTE OF ATOMIC ENERGY, BEIJING)

The evaluation of the neutron capture cross section of $^{23}Na$ is of considerable importance to the liquid metal fast breeder reactor design and its safe operation. Moreover, Sodium is an important reference material, it can be combined with many other elements to form highly pure salts. And the evaluated data of this cross section could serve as a standard for many other cross section measurements and neutron flux measurement by employing sodium compound. For this reason, the measurement and evaluation of this cross section have been still followed with interest by ones to this day. The measurements[1~41] of the neutron capture cross section of $^{23}Na$ are listed in Table 1. From Table 1 it can be seen :

- Most of the measurements were carried out for the thermal neutrons, 24 keV neutrons and 14 MeV neutrons. The neutron radiative capture cross section data for other energy regions are quite sparse and the neutron resonance parameters should be adopted to describe the cross section behaviour in the resonance energy region.
- A few of the new experimental data are available. There are only two measurements for thermal neutrons[1,2] and one measurement for 14.7 MeV neutrons reported after 1980.

On the other hand, the " new" evaluated data available are those of ENDF / B–VI (distributed in January 1990) and IRDF–85. The evaluated data of ENDF / B–VI were converted from ENDF / B–V, and those of IRDF–85 were derived from the ENDF / B–V Dosimetry File directly. That means that the sourse of these data files is the same as ENDF / B–V. The evaluation of neutron capture cross section of $^{23}Na$ for ENDF / B–V was finished by D. C. Larson[42]. As a result ,we take a review to the data given by ENDF / B–VI as

the point of departure of our evaluation.

## $10^{-5}$ eV ~ 500 keV NEUTRON ENERGY REGION

In Larson's evaluation, resonance parameters were used from 600 eV to 500 keV. Using resonance parameters $E_0 = 2.81$ keV, $\Gamma_n = 376$ eV and $\Gamma_\gamma = 0.353$ eV for the large 2.81 keV resonance and Breit–Wigner formula the correct thermal capture value was given, and this form was used to calculate the capture cross section from $10^{-5}$ to 600 eV. The thermal capture cross section was given as 528 mb.In consideration of facts that no new experimental data of neutron resonance parameters concerned are available after 1980, and the selection of neutron resonance parameters in Larson's evaluation is still reasonable in the light of present point of view, we put our attention on reevaluation of the thermal neutron capture cross section. As shown in Table 1, there are more than 20 measurements for the thermal neutrons. In order to reduce the scope, we have taken those results with a quoted error of less than ± 3 % and made renormalizations for these data ( as listed in Table 2 ). The standard cross sections for thermal neutrons adopted in present evaluation are as follows :

$\sigma_\gamma(^{197}\mathrm{Au}) = 98.65 \pm 0.09$ b [43]

$\sigma_a(\mathrm{B}) = 761 \pm 3$ b for ANL – BNL Boron [44]

$773 \pm 3$ b for Harwell Boron[44]

A weighted average value of 0.527 ± 0 .006 b (where the error is external error ) for thermal neutron capture cross section of $^{23}$Na is obtained. This value is in agreement with that of ENDF / B–VI, but is a little lower than the recommended data given by Mughabghab ( 0.530 ± 0.005 b )[43] and Gryntakis et al. ( 0.530 ± 0.007 b )[45]. It is comprehensible because the lower new experimental value of 0.513 ± 0.0041 b[1] has taken in our evaluation into account. We believe that the value of 0.527 ± 0.006 b for thermal neutron capture cross section of $^{23}$Na is reasonable on the level of our present understanding. This shows that the evaluated data of ENDF / B–VI in $10^{-5}$ eV ~ 500 keV neutron energy region are acceptable too. Consequently, they are adopted in our evaluation .

## 0.5 MeV ~ 20 MeV NEUTRON ENERGY REGION

Comparing the ENDF / B–VI data with the experimental data, it can be seen, the ENDF / B–VI data are in good agreement with the experimental data in the neutron energy region from 0.5 to 0.9 MeV, and a obvious discrepancy exists in the high energy region. Especially, the trend of cross section curve of ENDF / B–VI is totally different from the experimental data given by

Menlove et al.[12] and Csikai et al.[11]. That is to say, according to the evaluated data given by ENDF / B–VI, the radiative capture cross section of $^{23}$Na increase with increasing neutron energy above 14 MeV region, however, the experimental data are tending to decrease. In order to judge what is the proper trend of the excitation curve, we make a systematics calculation by using a systematics formula[46] which is based on the statistical theory and exciton model. The calculation indicates that there is a giant resonance existed above 10 MeV and the cross section trend is tending to decrease above 14 MeV which is in good agreement with Menlove's data[12]. Fig. 1 shows the result of the systematics calculation compared with experimental data.

In view of this situation, a reevaluation based on the experimental data has been carried out.

Eight experimental data sets measured by Magnusson et al.[3], Sigg[5], Holub et al.[7], Csikai et al.[11], Menlove et al.[12], Bame Jr. et al.[22], Perkin[25] and Reese Jr. et al.[35] are selected and renormalized by using the new standard cross section. The new standards adopted are the evaluated data of ENDF / B–VI for $^{235}$U fission cross section in the neutron energy region from 500 keV to 20 MeV and the recommended data given by Vonach[47] for $^{27}$Al ( n,α) reaction cross section in 14 MeV neutron energy region. A data treatment code[48] is used to make the curve fitting with polynomial. Combining the fitted data in 0.9 to 20 MeV region with the ENDF / B–VI data in 0.5 ~ 0.9 MeV region, the evaluated data of neutron capture cross section of $^{23}$Na from 0.5 to 20 MeV are obtained and listed in appendix. A comparison of evaluated and measured data is shown in Fig. 2.

## COVARIANCE

Uncertainty files for the capture cross section are estimated from the experimental error and the spread in the various data sets.

They are estimated as :

2 % for $10^{-5}$~ 50 eV neutrons
5 % for 50 ~ 600 eV neutrons
10 % for 600 eV ~ 500 keV neutrons
20 % for 500 keV ~ 5 MeV neutrons
25 % for 5 ~ 20 MeV neutrons

## DISCUSSION

A comparison of measured and calculated spectrum – averaged neutron

capture cross section of $^{23}Na$[49~52] is presented in Table 3. The differential cross sections used for their calculations were taken from IRDF–82 or ENDF / B–V. As mentioned above, they are the same as those of ENDF / B–VI.

As can be seen from the table, the agreement between calculated and measured values is rather poor, and the values are contradictory each other for the different benchmark spectra. It shows that more precise knowledge of these spectra and further measurements are still needed. It looks as if our evaluation would be closer to Lamaze's value[51] than that of ENDF / B–VI.

## ACKNOWLEDGEMENTS

Thanks are due to Zhang Jin for his help in fitting data and to Liu Tong for his help in systematics calculation.

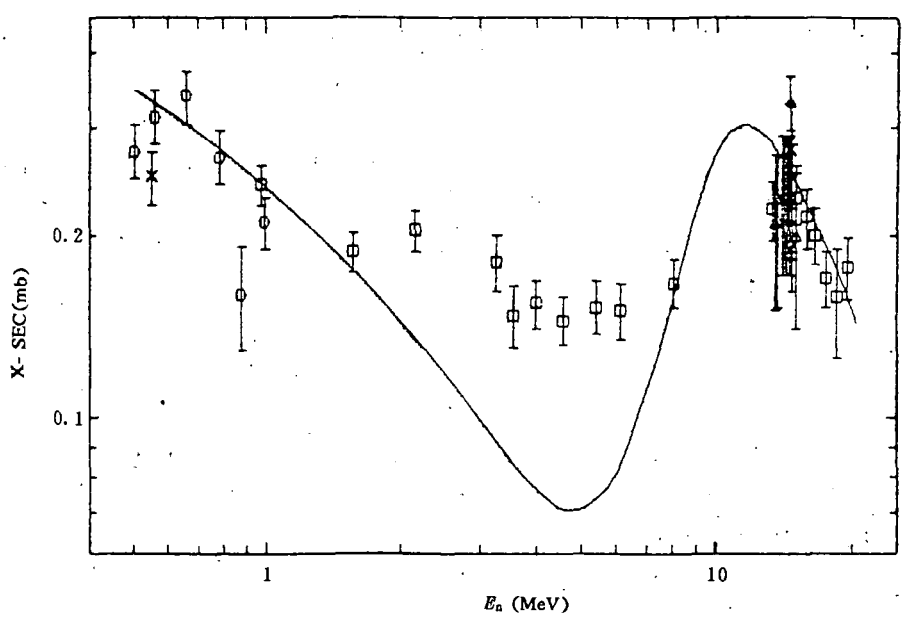


Fig.1 Systematics calculation of $^{23}Na(n,\gamma)$ reaction cross section compared with experimental data

□ Menlove(67) x Reese(53) ⋏ Sigg(76)
○ Bame(59) ◇ Holub(72) z Magnusson(82)
△ Csikai(67) ▲ Perkin(58) — Systematics calculation

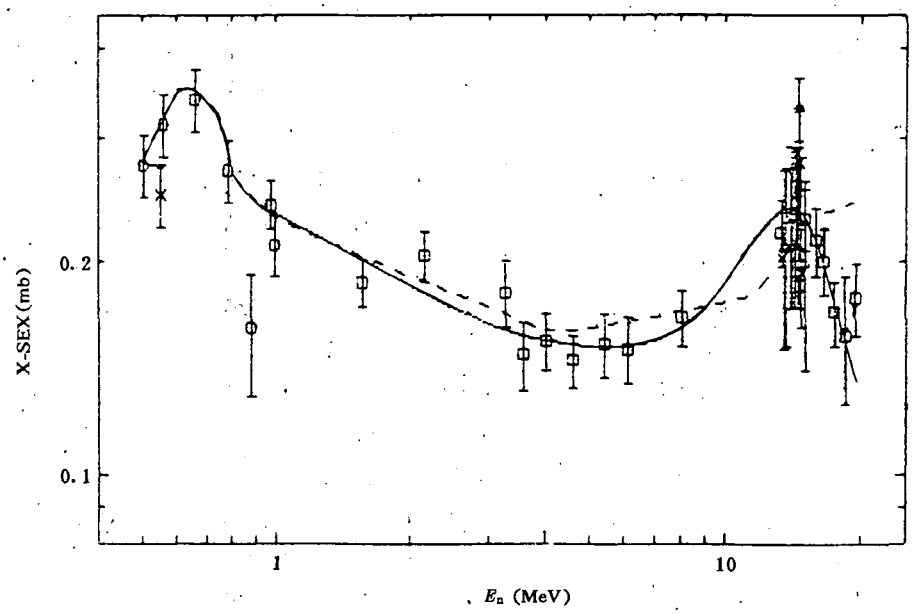


Fig.2 Comparison of evaluated and measured data

□ Menlove(67) x Reese(53) ⊼ Sigg(76) — Recommended Data

o Bame(59) ◇ Holub(72) z Magnusson(82) ---- ENDF / B-VI

△ (Sikai(67) ▲ Perkin(58)

**Table 1 Servey of experimental measurements for $^{23}Na(n,\gamma)^{24}Na$ cross section**

| Yr | Lab | Author | Points | Value &/or Range | Standard | Ref. |
|---|---|---|---|---|---|---|
| 88 | INW | De Corte+ | 1 | 0.513 b at thermal | $^{197}Au\ \sigma_{n,\gamma}$ | 1 |
| 82 | JPN | Kaminishi+ | 1 | 0.577 b at thermal | | 2 |
| 80 | LND | Magnusson+ | 1 | 0.190 mb at 14.70 MeV | $^{197}Au\ \sigma_{n,2n}$ | 3 |
| 78 | LRL | Heft | 1 | 0.523 b at thermal | | 4 |
| 76 | ARK | Sigg | 1 | 0.280 mb at 14.60 MeV | $^{27}Al\ \sigma_{n,\alpha}$ | 5 |
| 75 | OAU | Gleason | 1 | 0.54 b at thermal | $^{197}Au\ \sigma_{n,\gamma}$ | 6 |
| 72 | RBZ | Holub+ | 1 | 0.250 mb at 14.40 MeV | $^{56}Fe\ \sigma_{n,p}$ | 7 |
| 70 | NPL | Ryves+ | 1 | 0.527 b at thermal | $^{197}Au\ \sigma_{n,\gamma}$ | 8 |
| 70 | RPI | Yamamuro+ | 1 | 0.50 b at thermal | Cd $\sigma_{n,\gamma}$ | 9 |
| 68 | MUA | Hassan+ | 1 | 1.65 mb at 24.0 keV | $^{127}I\ \sigma_{n,\gamma}$ | 10 |
| 67 | DEB | Csikai+ | 1 | 0.240 mb at 14.7 MeV | $^{27}Al\ \sigma_{n,\alpha}$ | 11 |
| 67 | DEB | Csikai+ | 7 | 13.40 MeV to 15.00 MeV | | 11 |
| 67 | LOK | Menlove+ | 17 | 0.97 MeV to 19.39 MeV | $^{235}U\ \sigma_{n,f}$ | 12 |
| 66 | CAD | Le Rigoleur+ | 18 | 8.55 keV to 0.134 MeV | $^{7}Li\ \sigma_{n,t}$ | 13 |
| 64 | FEI | Bondarenko | 1 | at thermal | $^{235}U\ \sigma_{n,f}$ | 14 |
| 63 | ORL | Macklin+ | 2 | 30.0 keV to 65.0 keV | I $\sigma_{n,\gamma}$ | 15 |
| 63 | ROS | Alexander+ | 1 | 0.49 b at thermal | B $\sigma_{\alpha}$ | 16 |
| 63 | MUN | Koehler | 1 | 0.50 b at thermal | B $\sigma_{\alpha}$ | 17 |
| 62 | ROS | Wigner | 1 | 0.49 b at termal | | 18 |
| 61 | ANL | Meadows+ | 1 | 0.47 b at thermal | | 19 |
| 60 | MUN | Wolf | 1 | 0.531 b at thermal | $^{197}Au\ \sigma_{n,\gamma}$ | 20 |
| 59 | ORL | Lyon+ | 1 | 0.700 mb at 0.195 MeV | | 21 |
| 59 | LAS | Bame Jr.+ | 19 | 20.00 keV to 0.990 MeV | | 22 |
| 59 | HAR | Rose+ | 1 | 0.536 b at thermal | B $\sigma_{\alpha}$ | 23 |
| 58 | HAR | Jowitt+ | 1 | 0.536 b at thermal | B $\sigma_{\alpha}$ | 24 |
| 58 | ALD | Perkin+ | 1 | 0.330 b at 14.50 MeV | $^{3}H\ \sigma_{d,n}$ | 25 |
| 58 | FEI | Leipunskij+ | 3 | 0.200 MeV to 4.00 MeV | $^{127}I\ \sigma_{n,\gamma}$ | 26 |
| 58 | FEI | Kononov+ | 1 | 1.710 mb at 24.0 keV | $^{127}I\ \sigma_{n,\gamma}$ | 27 |
| 58 | LRL | Booth+ | 1 | 1.100 mb at 24.0 keV | $^{127}I\ \sigma_{n,\gamma}$ | 28 |
| 57 | ORL | Macklin+ | 1 | 1.000 mb at 24.0 keV | $^{127}I\ \sigma_{n,\gamma}$ | 29 |

| | | | | | | | | |
|---|---|---|---|---|---|---|---|---|
| 56 | HAR | Cocking+ | 1 | 0.536 | b | at thermal | $^{197}Au\ \sigma_{n,\gamma}$ | 30 |
| 55 | ORL | Brooksband+ | 1 | 0.50 | b | at thermal | $^{197}Au\ \sigma_{n,\gamma}$ | 31 |
| 55 | KJL | Grimeland | 1 | 0.51 | b | at termal | B $\sigma_{\alpha}$ | 32 |
| 53 | CRC | Bartholomew+ | 1 | 0.53 | b | at thermal | $^{197}Au\ \sigma_{n,\gamma}$ | 33 |
| 53 | ANL | Harris+ | 1 | 0.503 | b | at thermal | B $\sigma_{\alpha}$ | 34 |
| 53 | ORL | Reese Jr.+ | 1 | 0.25 | mb | 500 to 600 keV | | 35 |
| 52 | HAR | Littler+ | 1 | 0.494 | b | at thermal | B $\sigma_{\alpha}$ | 36 |
| 51 | ORL | Pomerance+ | 1 | 0.47 | b | at thermal | $^{197}Au\ \sigma_{n,\gamma}$ | 37 |
| 50 | HAR | Colmer+ | 1 | 0.50 | b | at thermal | B $\sigma_{\alpha}$ | 38 |
| 49 | ANL | Hughes+ | 1 | 0.26 | mb | at 1 MeV | $^{23}Na\ \sigma_{n,\gamma}$ | 39 |
| 47 | ANL | Seren+ | 1 | 0.63 | b | at thermal | | 40 |
| 47 | UI | Coltman+ | 1 | 0.47 | b | at thermal | B $\sigma_{\alpha}$ | 41 |

**Table 2 Measured thermal neutron cross section for $^{23}Na$**

| Author | (Yr) | Measured value, b | Adjusted value, b | Ref. |
|---|---|---|---|---|
| De Corte+ | (88) | 0.513 ± 0.0041 | 0.513 ± 0.0041 | 1 |
| Kaminishi+ | (82) | 0.577 ± 0.008 | 0.577 ± 0.008 | 2 |
| Ryves+ | (70) | 0.5269 ± 0.0045 | 0.526 ± 0.0045 | 8 |
| Wolf | (60) | 0.531 ± 0.008 | 0.531 ± 0.008 | 20 |
| Rose+ | (59) | 0.536 ± 0.008 | 0.540 ± 0.008 | 23 |
| Jowitt+ | (58) | 0.536 ± 0.008 | 0.539 ± 0.008 | 24 |
| Cocking+ | (57) | 0.536 ± 0.006 | 0.536 ± 0.006 | 29 |
| Harris+ | (53) | 0.503 ± 0.005 | 0.507 ± 0.005 | 34 |
| Littler+ | (52) | 0.494 ± 0.015 | 0.538 ± 0.015 | 36 |
| Colmer+ | (50) | 0.500 ± 0.015 | 0.544 ± 0.015 | 38 |

**Table 3 Comparison of measured and calculated spectrum averaged cross sections for $^{23}Na$**

| Benchmerk spectra | Measured value, mb | Calculated value, mb |
|---|---|---|
| $^{252}Cf$ fiss (NBS) | 0.335 ± 0.015 [49] | 0.2712 [50] |
| ISNF (NBS) | 1.57 ± 0.10 [51] | 1.98 [52] |

## REFERENCES


[1] F. De Corte et al., Proc. Int. Conf. on Nuclear Data for Science and Technology, Mito, 30 May–3 June, 1988, p.583.

[2] K. Kaminishi et al., J. Appl. Phys., 21, 636 (1982).

[3] G. Magnusson et al., Physica Scripta, 21, 21 (1980).

[4] R. E. Heft, Proc. ANS Topical Conf. on Computer in Activation Analysis and Gamma–Ray Spectroscopy, Mayaguez, 3 Apr.–4 May, 1978, p.495.

[5] R. A. Sigg, Dissertation Abstracts, B 37, 2237 (1976).

[6] G. Gleason, Radiochem. Radioanal. letters, 23, 317 (1975).

[7] E. Holub et al., LNS–4–72, 1972.

[8] T. B. Ryves et al., J. Nucl. Energy, 24, 419 (1970).

[9] N. Yamamuro et al., Nucl. Sci. Eng., 41, 445 (1970).

[10] S. S. Hasan et al., Nuovo Cimento, B 58, 402 (1968).

[11] J. Csikai et al., Nucl. Phys., A95, 229 (1967).

[12] H. O. Menlove et al., Phys. Rev., 163, 1299 (1967).

[13] C. Le Rigoleur et al., J. Nucl. Energy, Part A / B, 20,67 (1966).

[14] I. I. Bondarenko et al., Atomnaja Energija, 17, 113 (1964).

[15] R. Macklin et al., Phys. Rev., 129, 2695 (1963).

[16] K. Alexander et al., Ann. der Physik, 12, 225 (1963).

[17] W. Koehler, Zeitschrift f. Naturforschung, A18, 1339 (1963).

[18] K. Wigner, Kernenergie, 5, 790 (1962).

[19] J. W. Meadows et al., Nucl. Sci. Eng., 9, 132 (1961)

[20] G. Wolf. Nucleonik, 2, 255 (1960).

[21] W. S. Lyon et al., Phys. Rev. 114, 1619 (1959).

[22] S. J. Bame Jr. et al., Phys. Rev. 113, 256 (1959).

[23] H.Rose et al., Prog. Nucl. Energy, Vol. 3, Ser. 1, 292 (1959).

[24] D. Jowitt et al., AERE–R / R–2516, 1958.

[25] J. Perkin et al., Proc. Phys. Society, 72, 505 (1958).

[26] A. J. Leipunskij et al., Proc. Second UN Conf. on the Peaceful Uses of Atomic Energy, Geneva, 1–13 Sept. 1958, Vol. 15, p. 50.

[27] V. N. Kononov et al., Atomnaja Energija, 5, 564 (1958).

[28] R. Booth et al., Phys. Rev., 112, 226 (1958).

[29] R. Macklin et al., Phys. Rev., 107, 504 (1957).

[30] S. J. Cocking et al., J. Nucl. Energy, 3, 70 (1956).

[31] W. A. Brooksbank et al., Proc. of Nuclear Science and Engineering Congress, Cleveland, 12–16 Dec. 1955, p.203.

[32] B. Grimeland, J. Nucl. Energy. 1, 231 (1955).

[33] R. M. Bartholomew et al., Can. J. Chem., 31, 204 (1953).

[34] S. P. Harris, ANL – 5031, 68, 1953.
[35] H. Reese Jr. et al., ORNL–CF–53–8–22, 1953.
[36] D. J. Littler et al., AERE–R / R–961, 1952.
[37] H. Pomerance, Phys. Rev., 83, 641 (1951).
[38] F. C. W. Colmer et al., Proc. Phys. Soc., A63, 1175 (1950).
[39] D. J. Hughes et al., Phys. Rev., 75, 1781 (1949).
[40] L. Seren et al., Phys. Rev., 72, 888 (1947).
[41] J. Coltman et al., Phys. Rev., 69, 411 (1946).
[42] D. C. Larson, ORNL–5662, 1980.
[43] S. F. Mughabghab, Neutron Cross Sections, Vol. 1, Neutron Resonance Parameters and Thermal Cross Sections, Academic Press, Inc., 1984.
[44] Yuan Hanrong, CNDC – 85011, p.56, 1986.
[45] E. Gryntakis et al., Handbook on Nuclear Activation Data,ed. by K.Okamoto, IAEA, Vienna, 1987, p.199.
[46] Zhao Zhixiang et al., Systematics of Excitation Functions for ( n,γ) Reaction, to be published.
[47] H. Vonach, Nuclear Data Standards for Nuclear Measurements, IAEA Technical Reports Series No. 227, 1983, p.59.
[48] Zhang Jin et al., A Data Treatment Code for Nuclear Data Evalua tion and Simultaneous Evaluation, to be published.
[49] Z. Dezsoe et al., Proc. Conf. on Neutron Physics, Kiev, 18 – 22 April 1987, Vol. 3, p. 32.
[50] D. E. Cullen et al., Nucl. Sci. Eng., 83, 497 (1983).
[51] G. F. Lamaze et al., Proc. Int. Conf. on Nuclear Data for Science and Technology, Mito, 30 May – 3 June 1988, p. 1033.
[52] J. A. Grundl et al., NBSIR 85 – 3155, 1986.

# THE EVALUATION OF $^{2}H(n,2n)^{1}H$ REACTION CROSS SECTION

Cai Dunjiu Zhuang youxiang Wang Zisheng Yu Baosheng

(CNDC, INSTITUTE OF ATOMIC ENERGY, BEIJING)

This evaluation is based on Huang's evaluation[1]. All the experimental data of $^2H(n,2n)$ reaction until 1990 were collected, analysed and fitted. The recommended values are compared with the ENDF / B–6.

## 1 EXPERIMENTAL DATA

When the low energy neutron acts on deuteron, probable reactions induced are as follows :

$$n + {}^2H \rightarrow n + {}^2H,$$
$$n+n+p - 2.22\ MeV,$$
$$\gamma + {}^3H + 6.257\ MeV;$$

Thus $\sigma_{n,tot} = \sigma_{n,n} + \sigma_{n,2n} + \sigma_{n,\gamma}$ . When $E_n > 3.339$ MeV, $\sigma_{n,\gamma} \approx$ several tens $\mu$b.

Because $^2H(n,2n)$ p is one of the simplest three nucleons reactions without Coulomb interaction, it is very significant for research after nuclear force and for test of nuclear theory. Deuterium also is one of the important fusion fuels, therefore (n,2n) data are useful to nuclear power development.

It is more difficult to measure the $^2H(n,2n)p$ reaction cross section. Up to now all the measured data of 12 laboratories have been collected from threshold to 22 MeV. The methods used in the measurements can be divided into two categories :

(1) to measure the two neutrons by means of large liquid scintillator[2~5] or TOF[6~9];

(2) to measure the proton with the aid of particle identification spectrometer [10~13].

The accuracies of all the measurements are not very high, because there are many correction factors in both methods. Near to the threshold, (n,2n) reaction cross section is small, the uncertainty is about 60%; at the energy region much far from the threshold the errors are ~ 7–10%. All the experimental data coincide with each other within their errors on the whole and link up one another.

## 2 RECOMMENDATION AND COMPARISON

The original data and errors of all the experiments were analysed and fitted on computer MICRO–VAX–II with orthogonal polynomial. The recommended values are listed in Table 1.

**Table 1 The recommended $^2H(n,2n)$ cross section**

| $E_n$(eV) | $\sigma_{n,2n}$(b) | $E_n$(eV) | $\sigma_{n,2n}$(b) | $E_n$(eV) | $\sigma_{n,2n}$(b) |
|---|---|---|---|---|---|
| 3.3390E+06 | 0.0000E+00 | 3.4000E+06 | 3.0920E−04 | 3.5000E+06 | 1.2320E−03 |
| 3.7500E+06 | 5.0700E−03 | 4.0000E+06 | 9.1640E−03 | 4.2500E+06 | 1.4390E−02 |
| 4.5000E+06 | 2.1420E−02 | 5.0000E+06 | 3.4960E−02 | 5.5000E+06 | 4.7790E−02 |
| 5.6000E+06 | 5.0280E−02 | 6.0000E+06 | 5.9940E−02 | 6.5000E+06 | 7.1400E−02 |
| 7.0000E+06 | 8.2200E−02 | 7.2500E+06 | 8.7360E−02 | 7.5000E+06 | 9.2360E−02 |
| 7.8500E+06 | 9.9090E−02 | 8.0000E+06 | 1.0190E−01 | 8.5000E+06 | 1.1080E−01 |
| 9.0000E+06 | 1.1910E−01 | 9.5000E+06 | 1.2680E−01 | 9.7000E+06 | 1.2970E−01 |
| 1.0000E+07 | 1.3400E−01 | 1.0500E+07 | 1.4060E−01 | 1.1000E+07 | 1.4660E−01 |
| 1.1500E+07 | 1.5210E−01 | 1.1750E+07 | 1.5470E−01 | 1.2000E+07 | 1.5710E−01 |
| 1.2170E+07 | 1.5870E−01 | 1.2250E+07 | 1.5940E−01 | 1.2500E+07 | 1.6160E−01 |
| 1.3000E+07 | 1.6570E−01 | 1.3500E+07 | 1.6920E−01 | 1.4000E+07 | 1.7230E−01 |
| 1.4100E+07 | 1.7290E−01 | 1.4500E+07 | 1.7500E−01 | 1.5000E+07 | 1.7730E−01 |
| 1.6000E+07 | 1.8060E−01 | 1.7000E+07 | 1.8230E−01 | 1.8000E+07 | 1.8270E−01 |
| 1.9000E+07 | 1.8190E−01 | 2.0000E+07 | 1.7980E−01 | | |

There are 10 measured data at $E_n \approx 14$ MeV, their average value is ~ 173 mb, which coincides with the recommended one.

Because the errors of experimental data are larger, the fitted errors given by orthogonal polynomial can't be taken as the recommended ones; thus the smallest error of experimental data in each energy region is regarded as the error of recommended values in this region, usually ~ 10%.

All the measured data, our evaluation, ENDF / B−6 and phase−shift analysis calculation of Fudan University [14] are shown in Fig. 1. It is thus evident that the values of ENDF / B−6 are larger than experimental data at $E_n > 10$ MeV, especially $E_n > 15$ MeV.

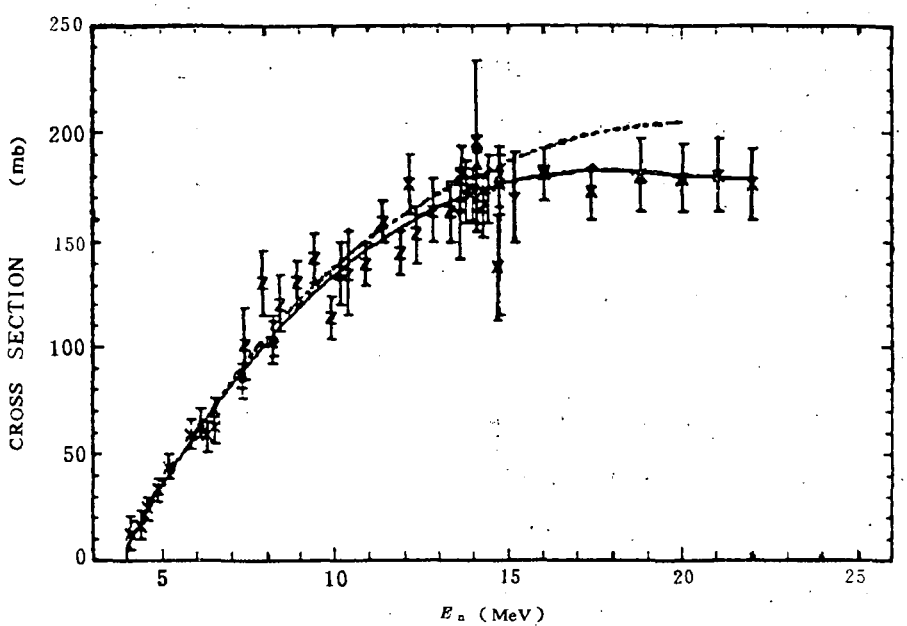


Fig. 1 The comparison between experimental and recommended data of $^2H(n,2n)$ reaction cross section

—V. J. Ashby (58) —E. R. Graves (71) — Shen Guanren (90)
—H. C. Catron (61) —N. Koori (72) — Bai Xixiang (80)
—S. S.hirato (68) —G. Pauletta (75) —G. Vedrenne (66)
—M. Holmberg (69) —J. Frehaut (85) —K. Gul (79)
— Present evaluation — • — Phase–shift analysis ····· ENDF / B–6

In general, $^2H(n,2n)$ reaction cross sections were measured from threshold to 22 MeV; however, their uncertainties are larger. Therefore more accurate measurements are necessary at important energy region.

## REFERENCES


[1] Huang Shengnian, The Compilation and Evaluation of $^{2}H(n,2n)$ Reaction Cross Section, hsj–77095(bp) 1978.

[2] V. J. Ashby et al., Phys. Rev., 111, 616(1958).

[3] H. C. Catron et al., Phys. Rev., 123, 218(1961).

[4] M. Holmberg, Nucl. Phys., A129, 327 & 305(1969).

[5] J. Frehaut et al., 85 Santa Fe, (B06), 1985.

[6] Shen Guan Ren et al., Chinese Journal of Nucl. Phys., 12, 3, 241(1990).

[7] Bai Xixiang et al., Chinese Journal of Nucl. Phys., 2, 4, 327(1980).

[8] K. Gul et al., J. Phys. G : Nucl. Phys., 5(8), 1107(1979).

[9] G. Vedrenne et al., Journal de physique(Colloque) 27(1) 71(1966) & 25, 678(1964) & 24, 801(1963); Nucl. Struct. Study with Neutrons, 510 (1965); LLL–ECSIL 76.

[10] S. Shirato et al., Nucl. Phys., A120, 387(1968) & NIM, 57, 325(1967).

[11] N. Koori et al., JPSJ, 32, 306(1972).

[12] E. R. Graves et al., NCSAC–42, 158(1971).

[13] G. Pauletta et al., Nucl. Phys., A255, 267(1975).

[14] Chen Jianxin et al., CNDP 4, (1990).


# THE EVALUATION OF $^{59}Co(n,\gamma)^{60}Co$ REACTION CROSS SECTION AND ITS COVARIANCE DATA


Liu Tong Zhou Delin

(CHINESE NUCLEAR DATA CENTER, IAE, BEIJING)


## INTRODUCTION

$^{59}Co(n,\gamma)^{60}Co$ reaction cross section is of importance for dosimetry application. The evaluation and its covariance for ENDF / B–V were performed by S. Mughabghab in 1977. Since then, there are no any newly measured data. Although the resonance parameters measured by Spencer et al.[1,2] was published before that of the evaluation for ENDF / B–V, only the data in the unresolved resonance region measured by Spencer and Macklin[1] were adopted in the evaluation for BNL – 325[3]. The present evaluation including the covariance is also carried out based on the same data body.

# 1 EVALUATION OF CROSS SECTION ( MF = 3 )

## 1.1 Cross Section of Thermal Energy Region ( $1.0\times10^{-5}\sim$ 1 eV )

No large differences exist among measured thermal cross sections. See Tab. 1. In order to agree with the resonance parameters, the value of 37.18 ± 0.6 b is adopted in this evaluation.

## 1.2 Cross Section of Unresolved Resonance Region ( <1 MeV )

Few of measured point–wise cross sections are in resonance region.For obtaining the evaluation the cross section must be calculated from the evaluated resonance parameters. In the present case, there are two sets of measured resonance parameters carried out by Spencer et al., one with Electron Linear Accelerator in Oak Ridge National Laboratory[1], and the other with the Van de Graaff accelerator in Kernforschungszentrum[2] .These two measurements should be considered as independent measurements, it is noted that :

(1) The 30 keV Maxwellian–average capture cross sections calculated with these two sets of resonance parameters are in agreement with each other.

(2) The resonance parameters of these two measurements are consistent essentially.

(3) These two sets of resonance parameters were adopted in the evaluation for BNL – 325.

According to the following principles the resonance parameter sets are modified in our evaluation.

(1) The resonances, for which the $2g\Gamma_n^o$ or $2g\Gamma_n$ are not given, are not adopted.

(2) The $J$ values are assigned randomly in proportion to the level density factor $2J+1$ to the resonances for which the $J$ values are not given.

(3) $L=1$ are assigned to the resonances for which $L$ values are not given.

(4) The averaged $\Gamma\gamma$ are given for the resonances for which the $\Gamma\gamma$ are not given, i. e.

$$<\Gamma\gamma> = 0.564\ \text{eV} \quad \text{for } J=3$$
$$<\Gamma\gamma> = 0.486\ \text{eV} \quad \text{for } J=4$$

The final resonance parameter set is used to calculate the point–wise cross sections for present evaluation by using the code MLEPT.

## 1.3 Cross Section of Unresolved Resonance Region (85 keV ~ 1 MeV)

The measured results of Spencer and Macklin[1] are adopted for this evaluation.

## 1.4 Cross Section in the Smooth Region

The excitation function of systematics predictions[4] in the smooth region is

adopted and normalized to 1.01 ± 0.13 mb, the average value of two measurments of M. Budnar and F. Rigaud at 14.1 MeV, see Tab. 2.

The results are shown in Fig. 1.

## 2 COVARIANCE ( MF = 33 )

1. An uncertainty of 2 % is given to the cross section in the thermal energy region.

2. An uncertainty of 10 % is given for the resonance region based on the following reason :

(1) A systematic uncertainty less than 5 % is given in the Spencer and Macklin's measurement.

(2) The 30 keV Maxwellian–average capture cross section calculated from the measured data of Spencer and Beer is in agreement with that of Spencer and Macklin.

(3) The systematics prediction is in agreement with the measured cross section.

3. An uncertainty of 30 % is given for the systematics predictions for the smooth energy region of < 4 MeV.

4. An uncertainty of 20 % is given for the energy region of > 4 MeV considering the uncertainty of the shape of systematics prediction and the uncertainty of the measured value at 14 MeV for normalization.

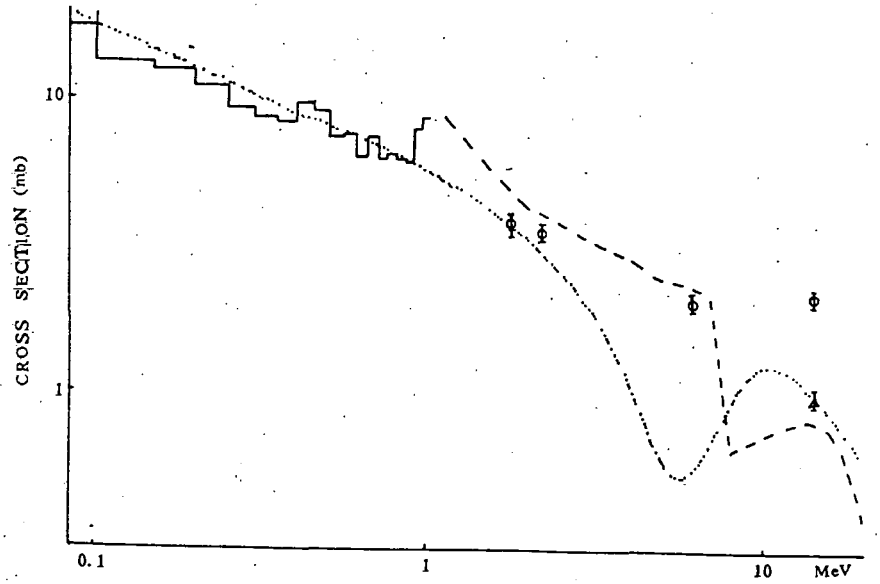


Fig. 1 Comparison of systematics prediction and ENDF / B–V

— P. R. Spence --- ENDF / B–V — • — • — Systematics

ϕ A. Paulsen Δ M. Budnar et al.

Table 1 **Measured and evaluated thermal cross sections( in barn )**

| | | | |
|---|---|---|---|
| 72 MOL | Deworm | DEWORM | 37.70 ± 0.4 |
| 69 HAR | Silk+ | AERE–R–6059 | 37.31 |
| 66 FAR | Carre+ | 66PARIS 1,479 | 38.00 |
| 61 ANL | Meadows+ | NSE 9,132 | 36.30 ± 0.6 |
| 61 BUC | Stefanescu+ | 61BUCHAR,553 | 38.40 ± 0.99 |
| 60 HAR | Tattersall+ | JNE / A 12,32 | 38.20 ± 0.7 |
| 52 FAR | Grimeland+ | CR 232,2089 | 33.90 |
| | ENDF / B–V | | 37.233 |
| | BNL–325 | | 37.18 ± 0.06 |
| | present work | | 37.18 ± 0.6 |

Table 2 **A survey of capture cross sections at the energy about 14 MeV**

| | | | | |
|---|---|---|---|---|
| 79 | M. Budnar | 1.005 ± 0.155 | mb | [6] |
| 71 | F. Rigaud | 1.02 ± 0.26 | mb | [5] |

## REFERENCES


[1] R. R. Spencer and R. L. Macklin, Nucl. Sci. Eng., 61, 346 (1976).

[2] R. R. Spencer and H. Beer, Nucl. Sci. Eng., 60, 390 (1976).

[3] S. F. Mughabghab, M. Divadeenam N. E. Holden Neutron Resonance Parameters and Thermal Cross Section, Part A: 1981.

[4] Zhao Zhixiang et al., Systematics of Excitation Function for ( n,γ) Reaction, to be published in Chinese Nucl. Phys.

[5] F. Rigaud, J. L. Irigaray and G. Y. Petit, Nucl. Phys., A173, 551, 1971.

[6] M. Budnar et al., INDC(YUG) – 6, 1979.

# SIMULTANEOUS EVALUATION FOR CORRELATED DATA OF THE FISSION CROSS SECTIONS OF $^{239}Pu$, $^{238}U$ AND $^{235}U$ AND THE CAPTURE CROSS SECTION OF $^{238}U$

Liu Tingjin Deng Jingshan

(CHINESE NUCLEAR DATA CENTER, IAE, BEIJING)

ABSTRACT

A way to construct the covariance matrices of the multi–set experimental data has been explored. The simultaneous evaluation for correlated data proposed in this paper has been applied to evaluate the cross sections of $^{239}Pu(n,f)$, $^{238}U(n,f)$, $^{238}U(n,\gamma)$ and $^{235}U(n,f)$ and the ratios, $R[\sigma_f(^{239}Pu)/\sigma_f(^{235}U)]$, $R[\sigma_f(^{238}U)/\sigma_f(^{235}U)]$ and $R[\sigma_\gamma(^{238}U)/\sigma_f(^{235}U)]$, and their covariance matrices were constructed. The consistent relations of different reaction cross sections and the correlations of experimental data have been taken into account in the evaluations.

## INTRODUCTION

Among the most important cross section required for nuclear engineering are the fission cross sections of $^{239}Pu$ $^{238}U$, $^{235}U$ and the capture cross section of $^{238}U$. Now there are many measurements of these quantities and their ratios to $^{235}U(n,f)$ cross section over the energy range 30 keV~20 MeV. It is necessary to critically collect and evaluate the available experimental data and to produce recommended cross sections with high accuracy and reliability.

The experiments are distinguished into two types, the absolute measurement and ratio measurement. The former includes the ratio measurements relative to all known standard cross sections such as H(n,n) and $^{10}B(n,\alpha)$, which have been measured more reliably than others. The latter

is the experiment performed relative to other reaction cross sections. These ratio data should be fully utilized in evaluation because they are more accurate than absolute ones.

The covariance matrices of experimental data are very important in nuclear engineering at present time. We have tried to find a way to construct the covariance matrix from the statistical property of experimental data. The covariance matrix includes all information of experimental errors, not only uncertainties but also the correlations.

Many evaluations for the cross sections of $^{239}$Pu(n,f), $^{238}$U(n,f), $^{238}$U( n,$\gamma$) and $^{235}$U(n,f) had been made. Most of them are isolated or individual evaluations, not considering the relations of different reactions and the correlations of experimental data. The present method, the simultaneous evaluation for correlated data, in which the consistent relations of different reactions are taken into account, overcomes the defects of individual evaluations. With this developed method the cross sections of $^{239}$Pu(n,f), $^{238}$U(n,f), $^{238}$U( n,$\gamma$) and $^{235}$U(n,f) have been evaluated and their correlation covariance matrices have been given.

## 1 EVALUATION FOR EXPERIMENTAL DATA

The computer system of cross section simultaneous evaluation has been built (Fig. 1).

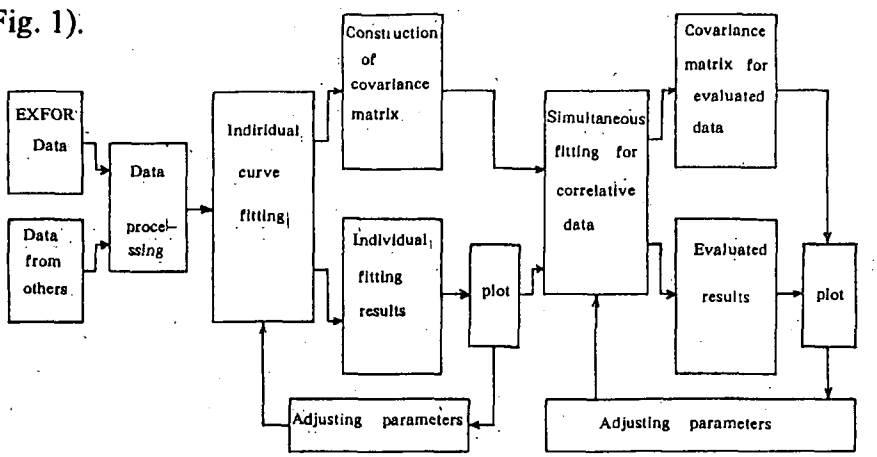


Fig. 1 The system of computer cross section simultaneous evaluation

169 sets of experimental data for $\sigma_f(^{239}\text{Pu})$, $\sigma_f(^{238}\text{U})$, $\sigma_\gamma(^{238}\text{U})$, $\sigma_f(^{235}\text{U})$, $R[\sigma_f(^{239}\text{Pu}) / \sigma_f(^{235}\text{U})]$, $R[\sigma_f(^{238}\text{U}) / \sigma_f(^{235}\text{U})]$ and $R[\sigma_\gamma(^{238}\text{U}) / \sigma_f(^{235}\text{U})]$ are chosen from the collected data.

1. Evaluation of $\sigma_f(^{239}\text{Pu})$ and $R[\sigma_f(^{239}\text{Pu}) / \sigma_f(^{235}\text{U})]$ 18 sets of experimental data for $\sigma_f(^{239}\text{Pu})$ and 21 sets for $R[\sigma_f(^{239}\text{Pu}) / \sigma_f(^{235}\text{U})]$ are chosen.

K. Kari[8] measured the $^{239}$Pu(n,f) cross section with recoil proton method

and TOF technique, using white light neutron source. The data above 9 MeV disagreed with others. So the data were divided into two parts at 9 MeV, and the smaller weight was given to the data above 9 MeV. I. Sarlea[9] and P. H. white[10] measured $^{239}$Pu(n,f) cross section relative to $^{235}$U(n,f) standard cross section. We turned the cross sections into ratio $R[\sigma_f(^{239}Pu) / \sigma_f^{235}U)]$ using the given $^{235}$U(n,f) cross sections. S. Cierjacks[11] measured the $^{239}$Pu(n,f) cross section relative to the $^{235}$U(n,f) cross section. The given errors were only for background. So the errors were corrected according to the measurement condition.

2. Evaluation of $\sigma_f(^{238}U)$ and $R[\sigma_f(^{238}U) / \sigma_f(^{235}U)]$ 18 sets of experimental data for the $^{238}$U(n,f) cross section and 28 sets for the ratio $R[\sigma_f(^{238}U) / \sigma_f(^{235}U)]$ were chosen.

In J. Blons's[12] experiment the white light neutron source and TOF technique were used. Only the data above 0.8 MeV were taken because below this energy the error was very large (up to 40%). In Osterhage's experiment ($\gamma$,n) neutron source was used. The neutron energy distribution is a Maxwell spectrum from 0.1 to 12.5 MeV with a peak around 2.0 MeV. The experimental data errors at both ends are bigger than usual, so only the experimental data from 1.5 to 8 MeV were taken.

3. Evaluation of $\sigma_\gamma(^{238}U)$ and $R[\sigma_f(^{238}U) / \sigma_f(^{235}U)]$ 24 sets of experimental data for the $^{238}$U( n,$\gamma$) cross section and 20 sets for the ratio $R[\sigma_\gamma(^{238}U) / \sigma_f(^{235}U)]$ were chosen.

M. Linder[13] measured the $^{238}$U(n,$\gamma$) cross section relative to the $^{235}$U(n,f) cross section (taken from ENDF / B–4). The $^{238}$U( n,$\gamma$) cross section was turned into the ratio $R[\sigma_\gamma(^{238}U) / \sigma_f(^{235}U)]$ by us. W. Poenity[14] measured the $^{238}$U( n,$\gamma$) cross section relative to $\sigma_f(^{235}U)$. With the given $^{235}$U(n,f) cross section we turned them into the ratio $R[\sigma_\gamma(^{238}U) / \sigma_f(^{235}U)]$.

4. The $^{235}$U cross section is an important cross section for nuclear reactor, and is often used as the standard one in the relative measured. 50 sets of experimental data were chosen.

W. K. Wrown's[15], L. W. Weston's[16] and E. Mignecd's[17] experimental data were averaged over every three or four energy points to decrease the energy point number, G. N. Smirenkin's[18] data were renormalized at 2.5 MeV energy point and the error was taken as $\sqrt{(0.01)^2 + (0.03)^2} = 3.16\%$ at this point. At other points the errors were taken as 5% according to usual measurement condition.

## 2 DATA PROCESSING METHOD

### 2.1 Spline Curve Fitting for Individual Reaction With Knot Optimization[5]

With the program SPF of the multi-set data spline fitting, above seven evaluated groups of experimental data for $\sigma_f(^{239}Pu)$, $\sigma_f(^{238}U)$, $\sigma_\gamma(^{238}U)$, $\sigma_f(^{235}U)$, $R[\sigma_f(^{239}Pu / \sigma_f(^{235}U)]$, $R[\sigma_f(^{238}U) / \sigma_f(^{235}U)]$ and $R[\sigma_\gamma(^{238}U) / \sigma_f(^{235}U)]$ are fitted respectively by 3-order spline function through adjusting initial knots and $\Sigma_k$ and optimizing the knots automatically to make $\chi^2$ smaller. In the fitting, the width for each set of data, $\Sigma_k$ , were taken very smaller ($10^{-4} \sim 10^{-7}$B) so that the errors of fitted values could be considered as only statistical ones[6]. The fitting result of $R[\sigma_f(^{238}U) / \sigma_f(^{235}U)]$ is shown as an example in Fig. 2.

### 2.2 Construction of Covariance Matrices for Experimental Data

Suppose for experimental data there is a systematical error $S_m$ which could make the data correlative. So the covariance matrices will be constructed with it. The procedures to get $S_m$ is shown as follows :

(a) To divide the whole energy range (30 keV ~ 20 MeV) into many intervals according to the situation of the data discrepancy.

(b) To count all experimental points ($N_m$) in the $m$-th interval ($m = 1,2,...,M$), and draw two lines, $L_1$ and $L_2$, which are parallel to the fitted

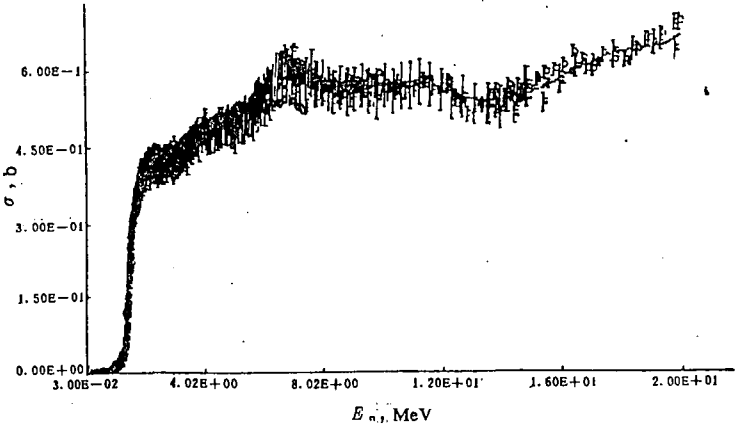


Fig. 2 The individual fitting curve of $R[\sigma_f(^{238}U) / \sigma_f(^{235}U)]$

## 3 RESULTS AND DISCUSSION

Using the simultaneous evaluation method for correlative data discussed above, four cross sections and their covariance matrix were given, which are consistent and correlative with each other. The results are shown in Figs. 4~7.

### 3.1 Comparing Between the Results of Simultaneous Evaluation for Correlative Data, Simultaneous Evaluation for Independent Data and Individual Evaluation

The comparison are shown in Figs. 4~7. The simultaneous fitted curves for independent data disagree with individual fitted curves at high energy intervals. These are as a result of adjusting of multi-curves to make them consistent.

curve on both sides of it. The number of the data points on the outsides of $L_1$ and $L_2$ is 31.7% $N_m$ / 2 respectively.

(c) To measure the distance between $L_1$ and $L_2$, the half of it is that $S_m$ (exactly, the experimental statistical error should be substracted from it), which characterize the systematic error of the individual fitting curve and the correlation of the experimental data of this interval.

Fig. 3 is an example to obtain $S_{11}$ of the 11–th interval (3～ 5 MeV) of $\sigma_f(^{235}U)$. There are 13 sets of experimental data and 104 data points in this interval. Between $L_1$ and $L_2$ there are 72 points. Out of $L_1$ and $L_2$ there are 16 points respectively. The half of the distance between $L_1$ and $L_2$, $S_{11}$, was 0.03798B.

According to above steps, $S_m$ of every energy interval for each curve were got.

From the statistical errors $\Delta\sigma_j$ $(j=1,2,...,N_E)$ and $S_m$ got in above way for each fitted curve, the covariance matrices can be constructed :

$$V_{ij}=\begin{cases} S_m^2+\Delta\sigma_i^2 & (i=j,\ i \text{ in the } m-\text{th interval}) \\ S_m S_n & (i\neq j,\ i \text{ in the } m-\text{th interval} \\ & \quad j \text{ in the } n-\text{th interval}) \end{cases}$$

The constructed matrices were very large because of the large number of energy points $N_E$. To make the matrices smaller take average of every 3 or 4 energy points for cross sections and statistical errors $\Delta\sigma_j$. In this way seven covariance matrices for $\sigma_f(^{239}Pu)$, $\sigma_f(^{238}U)$, $\sigma_\gamma(^{238}U)$, $\sigma_f(^{235}U)$, $R[\sigma_f(^{239}Pu)/\sigma_f(^{235}U)]$, $R[\sigma_f(^{238}U)/\sigma_f(^{235}U)]$ and $R[\sigma_\gamma(^{238}U/\sigma_f(^{235}U)]$ were constructed respectively (Suppose no correlation exists between curves).

### 2.3 Simultaneous Fitting for Multi–Curves

(1) Basic idea[7]

Take Logarithm of $N$ fitted cross section $\sigma_i'$ and $M$ fitted ratios $R_m'(=\sigma_i'/\sigma_j')$

$$\sigma_i=\ln\sigma_i' \qquad R_m=\ln R_m'=\ln\sigma_i'-\ln\sigma_j' \qquad (1)$$

Where $i,j=1,2,\cdots,N_j$ $m=1,2,\cdots,M$.

Turn $\sigma_i$ and $R_m$ into a multi–dimension vector :

$$Y=(\sigma_1,\sigma_2,\cdots,\sigma_N;\ R_1,R_2,\cdots,R_M) \qquad (2)$$

According to the least squares method :

$$\hat{C}=(B^T V_y^{-1} B)^{-1} B^T V_y^{-1} Y \tag{3}$$

$$V_{\hat{c}}=(B^T V_y^{-1} B)^{-1} \tag{4}$$

$$\hat{Y}=B\hat{C} \tag{5}$$

$$V_{\hat{y}}=B' V_{\hat{c}} B'^T \tag{6}$$

Where $B$ is the design matrix relative to spline base function. $\hat{C}$ is fit coefficient vector. $\hat{Y}$ is the vector for fitted values, $V_{\hat{y}}$ is the covariance matrix for evaluated data $\hat{Y}$. $V_y$ is :

$$\begin{bmatrix} V_1 & 0 & \cdots & \cdots & \cdots & 0 \\ 0 & V_2 & 0 & \cdots & \cdots & 0 \\ 0 & \cdots & \cdots & \cdots & \cdots & \cdots \\ 0 & 0 & V_N & 0 & \cdots & 0 \\ 0 & \cdots & 0 & U_1 & 0 & \cdots \\ 0 & \cdots & \cdots & 0 & U_2 & 0 \\ \cdots & \cdots & \cdots & \cdots & \cdots & \cdots \\ 0 & \cdots & \cdots & \cdots & \cdots & U_M \end{bmatrix} \tag{7}$$

Where diagonal matrices are the constructed covariance matrices for each cross sections and ratios.

(2) Fitting Parameters

With the program of the simultaneous evaluation for correlative data[7], seven individual fitted curves were fitted simultaneously again. The spline knots were basically taken as the same as ones of individual fitting, but slightly adjusted if it is needed. The weights of each curves were changed according to their reliability. In fact, the weights for ratios were adjusted larger because of their higher reliability.

In order to analyze and compare the results, the simultaneous evaluation for independent data was also done, for which the covariance matrices are fully diagonal.

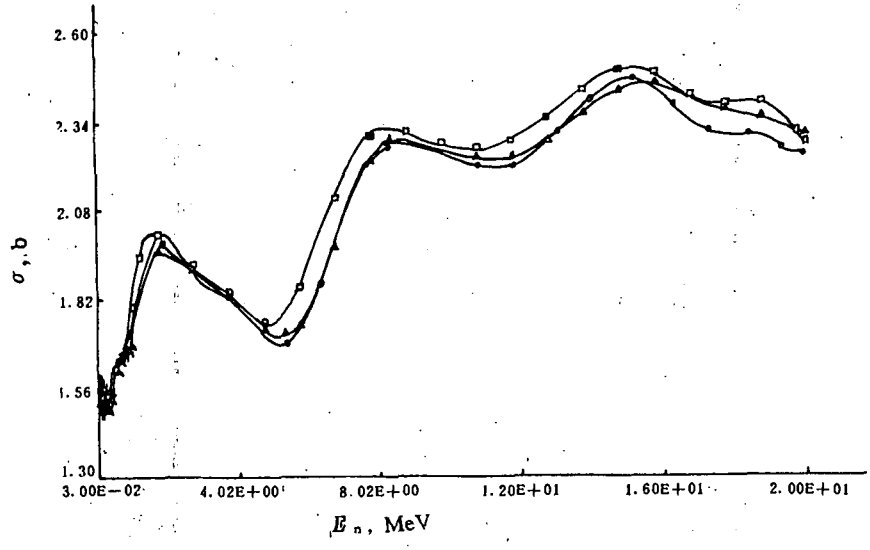


Fig. 3 An example to get systematical error :
$S_{11}$, the 11−th interval of $\sigma_f(^{235}U)$

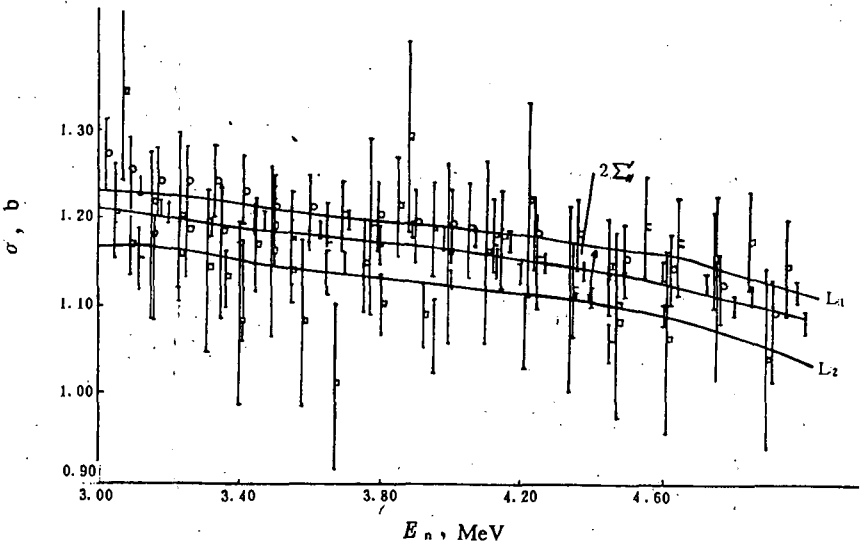


Fig. 4 The fitted cross section curve for $\sigma_f(^{239}Pu)$

—●— individual fitting curve

—▲— simultaneous evaluation for correlative data

—□— simultaneous evaluation for independent data

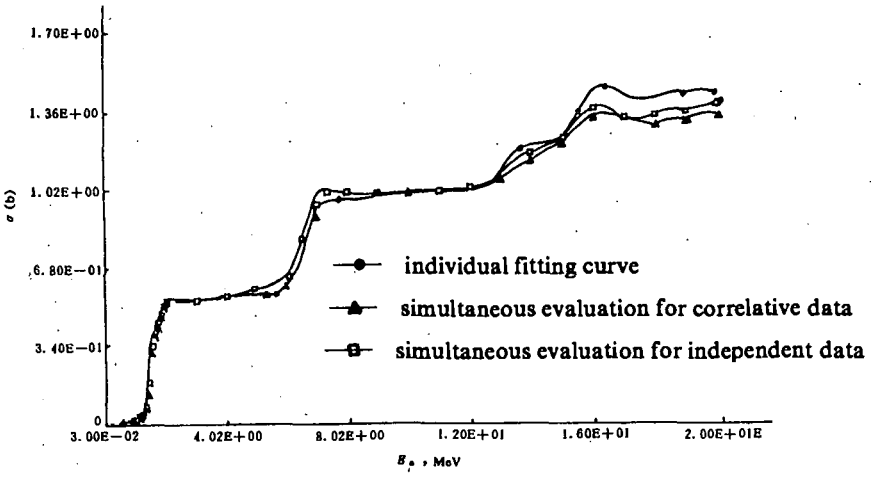


Fig. 5 The fitted cross section curve for $\sigma_f(^{238}U)$

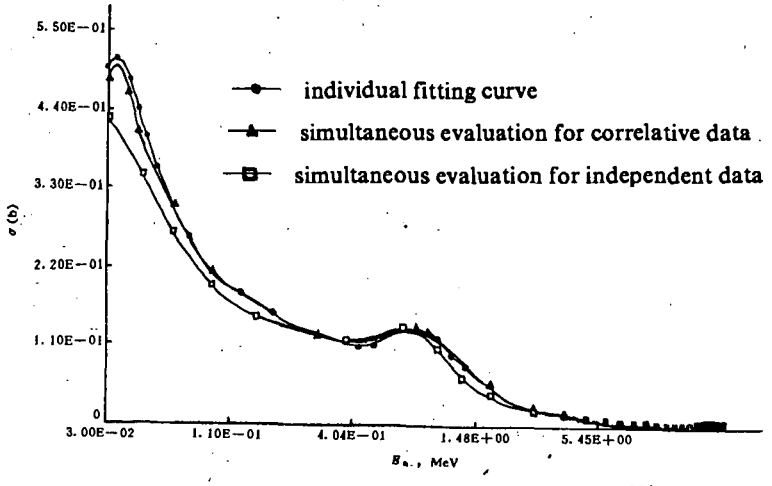


Fig. 6 The fitted cross section curve for $\sigma_{n,\gamma}(^{238}U)$

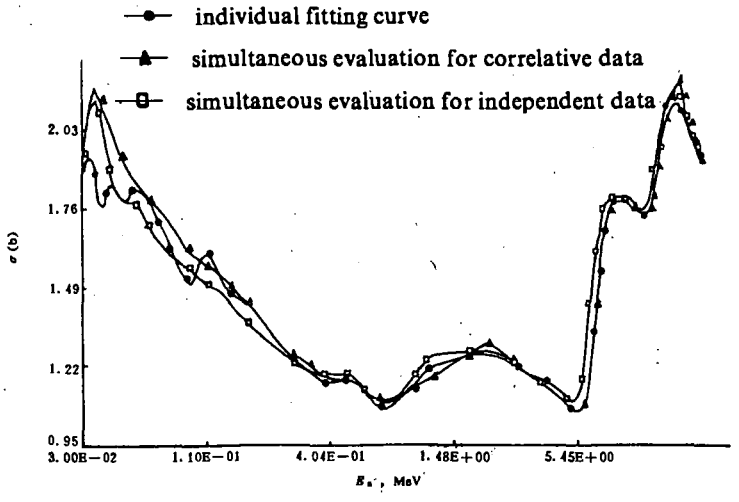


Fig. 7 The fitted cross section curve for $\sigma_f(^{235}U)$

The simultaneous fitted curves for correlated data roughly parallelly move to one side comparing with the simultaneous fitted curves for independent data. This may be caused by the data correlation.

### 3.2 Comparison of the Present Results with Other Evaluations

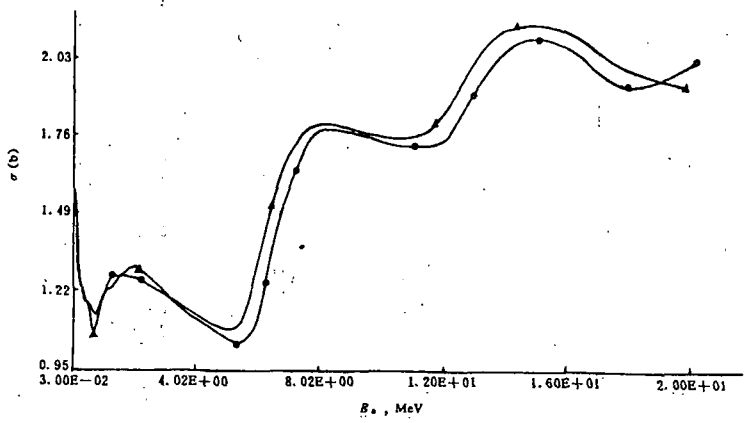


Fig. 8 The comparison between the present evaluation and ENDF / B−5 for $\sigma_f(^{235}U)$

present evaluation — ENDF / B−5

Fig. 8 shows the difference between present evaluated curve and ENDF / B−5 curve for $\sigma_f(^{235}U)$ at high energy range. The reason is that the $^{235}U(n,f)$ cross section curves recommended by ENDF / B−5 are the results of individual evaluation, not adjusting for consistent of different measurement. Fig. 8 also shows the parallel move of our present curve relative to ENDF / B−5 curve, which is caused by data correlation introduced in our evaluation.

Fig. 9 also shows the parallel move of our present fitted curve relative to Y. Uenohara's (Japan)[1~3] curve for $^{235}U(n,f)$ cross section, which is the result of the simultaneous evaluation for independent data by Y. Uenohara. This is caused by data correlation introduced in our evaluation.

Fig. 10 and 11 show the comparison of the present results with Liang Qichang's[19] evaluation for $\sigma_f(^{239}Pu)$ and Tang Guoyou's[20] for $\sigma_f(^{238}U)$. The experimental data used by Liang and Tang are as new as ours, but their recommended curves are the results of individual evaluation, not considering the consistent relations of different reaction cross sections and not introducing data correlation matrices, which is the reason for existing some difference between ours and theirs.

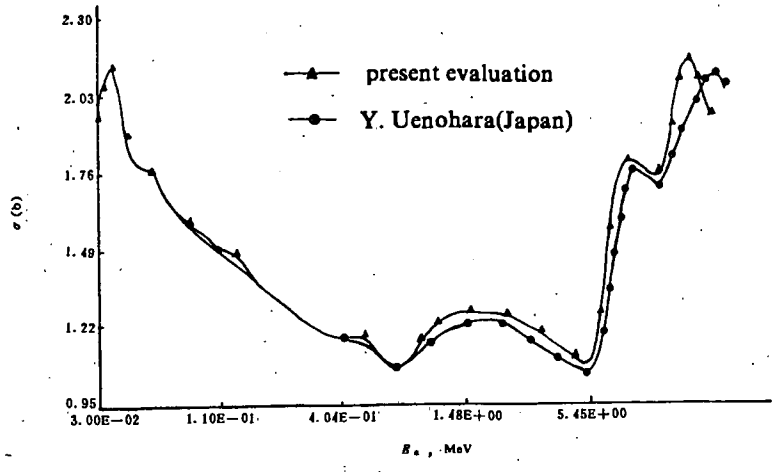


Fig. 9 The comparison between present evaluation and Y. Uenohara's for $\sigma_f(^{235}U)$

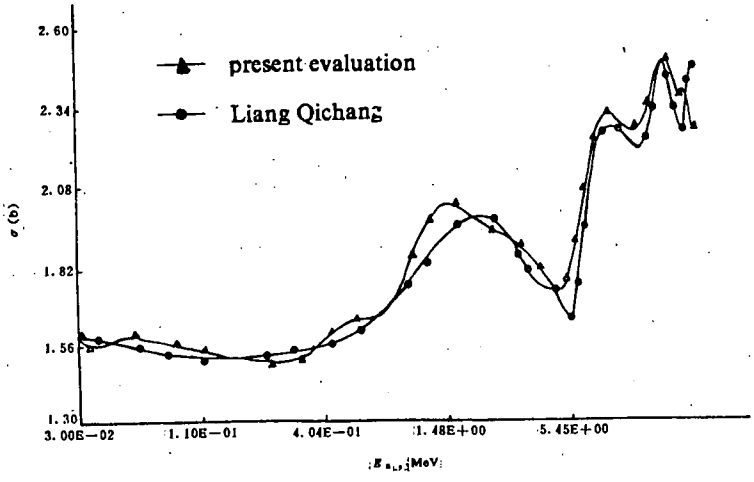


Fig. 10 The comparison between present and Liang's evaluation for $\sigma_f(^{239}Pu)$

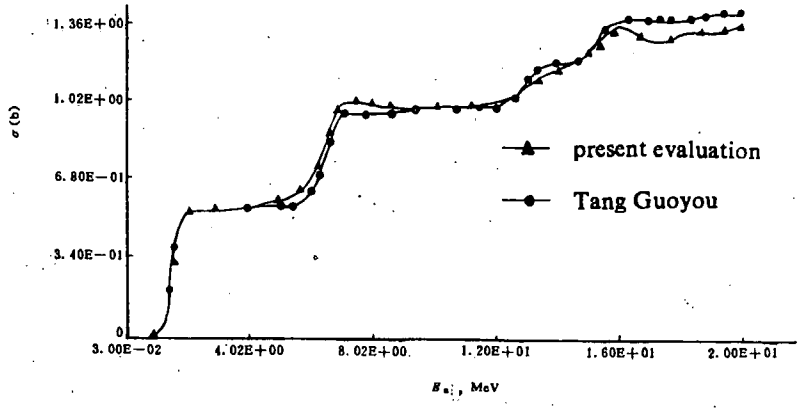


Fig. 11 The comparison between present and Tang's evaluation

### 3.3 The Covariance Matrix for Simultaneously Evaluated Data

30 output energy points were chosen to decrease the order of the covariance matrix because the number of the output points does not influence the correlated coefficients[4]. The output matrix is divided as follows :

$$\begin{bmatrix} A & B & C & D \\ & E & F & G \\ & & H & I \\ & & & J \end{bmatrix}$$

Where the diagonal matrices $A$, $E$, $H$ and $J$ are the covariance matrices of four evaluated cross sections themselves for $^{239}$Pu(n,f), $^{238}$U(n,f), $^{238}$U(n,$\gamma$) and $^{235}$U(n,f). Each of nondiagonal matrices $B$, $C$, $D$, $F$, $G$ and $I$ is covarcance matrix between $\sigma_f(^{239}Pu)$ and $\sigma_f(^{238}U$, $\sigma_f(^{239}Pu)$ and $\sigma_\gamma(^{238}U)$, $\sigma_f(^{239}Pu)$ and $\sigma_f(^{235}U)$, $\sigma_f(^{238}U)$ and $\sigma_\gamma(^{238}U)$, $\sigma_f(^{238}U)$ and $\sigma_f(^{235}U)$, $\sigma_\gamma(^{238}U)$ and $\sigma_f(^{235}U)$ respectively.

(1) The evaluated data covariance matrices for each reaction, $A$, $E$, $H$ and $J$

As an example, Fig. 12 shows the two points correlation with others for

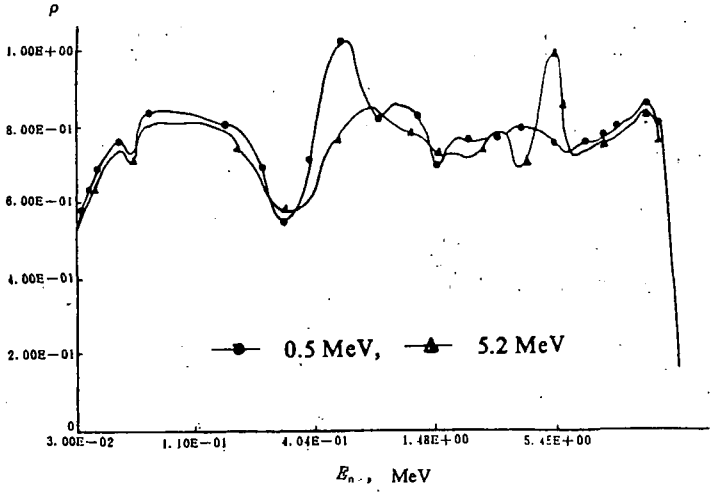


Fig. 12 The correlation for evaluated $^{239}$Pu(n,f) cross section

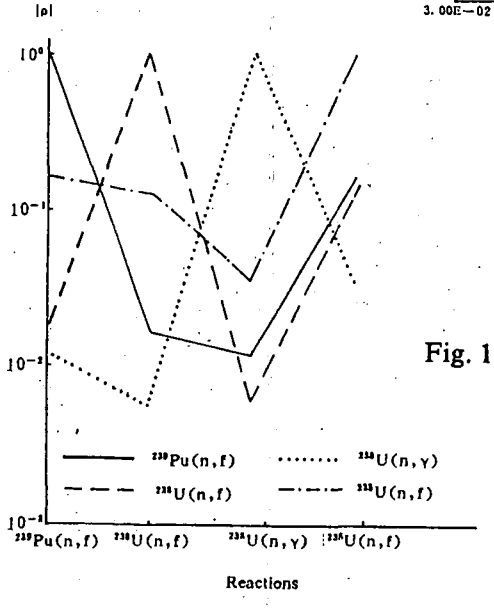


Fig. 13 The correlation coefficient of the different reactions at the same energy point (17 MeV)

$\sigma_f(^{239}Pu)$. From Fig. 12 it can be seen that the correlation coefficients at the same points of a reaction are 1, this is the inevitable result in physics. The correlation coefficients with other points are roughly as the same as input ones except nearby points, for which are larger.

(2) The correlation coefficients at same point for different reactions

As an example, Fig. 13 shows the correlation coefficients of different reactions at the same energy point. It can be seen that the correlation coefficients with $\sigma_f(^{235}U)$ are larger than others (the reason is that $^{235}U(n,f)$ cross section is used as "standard"), and the correlation coefficients between two reactions become larger if their cross sections are larger. Possibly because the bigger cross sections contribute more to simultaneous fitting in adjusting of cross sections and ratios.

(3) The correlation covariance matrices at different points for different reactions, *B*, *C*, *D*, *F*, *G* and *I*

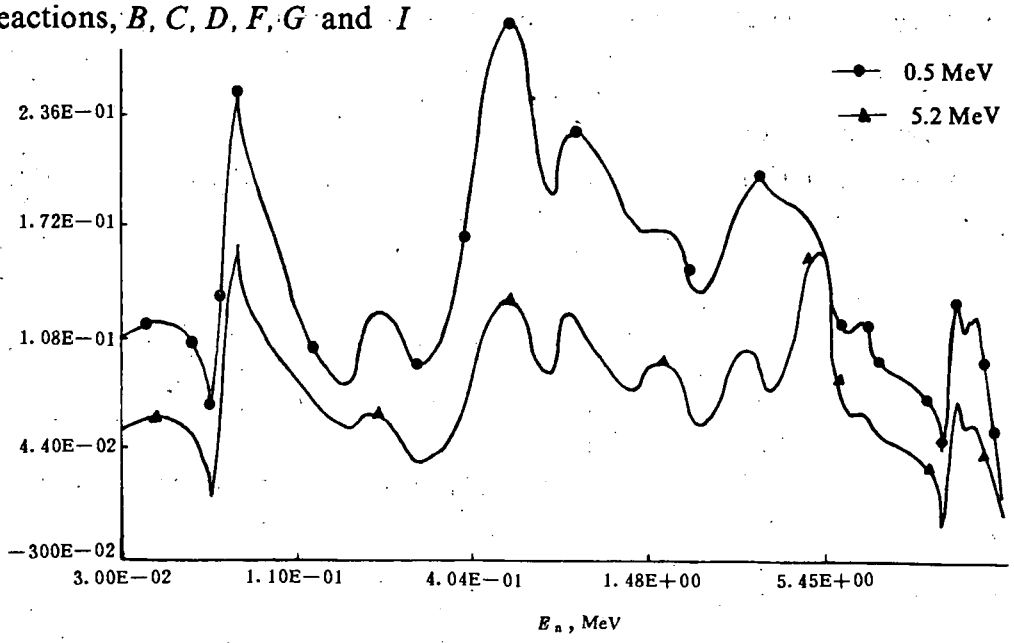


Fig. 14 The correlation coefficient between $^{239}Pu(n,f)$ and $^{235}U(n,f)$ at different energy points

As an example Fig. 14 shows the correlation between $\sigma_f(^{239}Pu)$ and $\sigma_f(^{238}U)$. It can be seen that the correlation coefficients for different energy points are smaller than that at the same energy points. There are positive correlation and negative correlation, which can be explained as following : If the fitted data $R=\sigma_i/\sigma_j$ increases, either $\sigma_i$ increases, or $\sigma_j$ decrease, then correlation between $\sigma_i$ and $\sigma_j$ is negative; or, if $\sigma_i$ increase faster than $\sigma_j$ , then correlation between $\sigma_i$ and $\sigma_j$ is positive. It can be explained in the same way if the fitted data $R=\sigma_i/\sigma_j$ decreases.

## 4. CONCLUSION

The methods and programs have been developed for construction of the covariance matrices of experimental data and for simultaneous evaluation for correlated data. The simultaneous evaluation for correlation data is an advanced method, it introduces the consistent relations of different reaction cross sections by ratios and the correlation of experimental data, and overcomes the defects of individual evaluation.

As the newly measured experimental data and more advanced methods have been used in the present evaluation so the recommended cross sections for $^{239}$Pu(n,f), $^{238}$U(n,f) $^{238}$U(n,$\gamma$), and $^{235}$U(n,f) with their correlation covariance matrices are more reasonable and reliable.

The authors express their appreciation to Drs. Liang Qichang (Chinese Nuclear Data Center, IAE), Tang Guoyou (Peking Univ.) for their discusion on the evaluations of $\sigma_f$($^{239}$Pu, $^{238}$U) and $\sigma_{n\gamma}$($^{238}$U), Chen Baoqian, Li Shubing (Nankai Univ.) for their help in computer program and Liu Jianfeng, Zhang Xizhi, Lu Zuhui (Zhengzhou Univ.) for their benefit advices.

## REFERENCES

[1] Y. Uenohara, Y. Kanda, Nuclear Data for Science and Technology, p169(1982).

[2] Y. Uenohara, Y. Kanda, Journal of Nuclear Science and Technology, 20, 787(1983).

[3] Y. Uenohara, Y. Kanda, INDC–46(1983).

[4] Liu Tingjin, Atomic Energy Science and Technology 24(1), 15(1990). (in Chinese).

[5] Liu Tingjin, Communication of Nuclear Data Progress Vol. 2, 58(1989).

[6] Liu Tingjin, Atomic Energy Science and Technology, 20 (3), 291(1986). (in Chinese).

[7] Liu Tingjin et al., Mathematical Treatment and Program for Simultaneous Evaluation (to be published).

[8] K. Kari et al., Meeting on Nucl. Data of Higher Pu and Am Isotopes for Reactor Applications, BNL(1978).

[9] I. Salea et al., Rev. Roum. Phys. 29, 421(1984).

[10] P. H. white et al., Proc. of Conf. on the Phys. and Chem. of Fission, Salzburg, Austria, 1, 219(1965).

[11] S. Cierjacks et al., Proc. of Meeting on Fast Neutr. Cross Sections of $^{233}$U, $^{235}$U, $^{238}$U and $^{239}$Pu, Argonnc, 94(1976).

[12] J. Blons et al., Phys. Rev. Lett., 35, 1749(1975).

[13] M. Linder et al., Nucl. Sci., Eng., 59, 381(1976).

[14] W. Poenitz et al., Proc. of Conf. on Develop. in Reactor Phys., Kiamesha Lake, New York, 2, 1107(1972).
[15] W. K. Wrown, Nucl. Sci. Eng., 2, 791(1966).
[16] L. W. Weston et al., Nucl. Sci. Eng., 88, 567(1984).
[17] E. Mignecd, Proc. of Conf. Nucl. Cross Sections and Technology, Washington D. C., 607(1975).
[18] G. N. Smirenkin, Atom. Ener., 13, 366(1962).
[19] Liang Qichang, Private Communication, 1990.
[20] Tang Guoyou, Private Communication, 1990.

# IV DATA PROCESSING

## ANALYSIS OF RESONANCE CROSS SECTION BY MEANS OF CORRECTED SLBW WITH MULTILEVEL EFFECT

Lu Guoxiong Qiu Guochun

(DEPARTMENT OF PHYSICS, GUANGXI UNIVERSITY)

Resonance cross section of $^{235}U$ was analysed by corrected SLBW formula with multilevel effect. We have obtained the interference parameters of 50 resonance levels below 30 eV and proposed a simple modified method in order to optimize the parameters so that the integral error of resonance cross section is below 1%.

### INTRODUCTION

Since the middle of this century, several multilevel formulas have been developed[1]for representation of the resonance cross section of heavy elements. In recent years, the single level Breit–Wigner formula with multilevel effect is proposed[2,3]. The characteristics of this formula aroused our interest. It is well known that the single level Breit–Wigner formula (i.e. SLBW) is simple in form and is used widely in analysis of the neutron cross section for various nuclei. A large number of SLBW parameters have already been evaluated for many nuclei. The SLBW parameters have been adopted usually in the calculation of resonance integral and rich experience have been obtained. SLBW only can represents the main properties of the resonance cross section for fissile nuclei and can not represent the interference effect between levels. An additional term is included in the traditional SLBW as the corrected formula. This is a new attempt to represent resonance cross sections in which interference between levels existed.

We have analysed the $^{235}U$ fission cross section with the corrected formula,

and proposed a simple modified method in order to optimize the parameters and obtained interference parameters for 50 levels below 30 eV. It may be seen that the corrected formula can reproduce precisely the neutron cross sections.

## 1 MULTILEVEL EXPANSION

According to R–Matrix theory, the collision matrix can be expressed in terms of the level matrix[4]:

$$U_{cc'} = \exp[-i(\varphi_c + \varphi_{c'})][\delta_{cc'} + i\sum_{\lambda\lambda'}\sqrt{(\Gamma_{\lambda c}\Gamma_{\lambda' c'})}A_{\lambda\lambda'}] \quad , \tag{1}$$

where $A$ is the level matrix. Its reciprocal matrix is

$$A^{-1}_{\lambda\lambda'} = (E_\lambda - E)\delta_{\lambda\lambda'} - (i/2)\sum_c\sqrt{(\Gamma_{\lambda c}\Gamma_{\lambda' c})}. \tag{2}$$

The summation over $c$ is understood over all reaction channels.

If $A^{-1}$ is rewritten as diagonal and off–diagonal parts, i.e.

$$A^{-1} = D + N,$$

therefore,

$$A = (D+N)^{-1} = D^{-1} - D^{-1}ND^{-1} + D^{-1}ND^{-1}ND^{-1} + \cdots.$$

Assuming $|N/D| << 1$, in the first order approximation,

$$A \approx D^{-1} + D^{-1}ND^{-1}$$

where

$$A_{\lambda\lambda'} = \delta_{\lambda\lambda'}/Z_\lambda + (i/2)(1-\delta_{\lambda\lambda'})G_{\lambda\lambda'}/Z_\lambda Z_{\lambda'}, \tag{3a}$$

$$Z_\lambda = (E_\lambda - E) - (i/2)\Gamma_\lambda, \tag{3b}$$

$$G_{\lambda\lambda'} = \sum_c\sqrt{(\Gamma_{\lambda c}\Gamma_{\lambda' c})}. \tag{3c}$$

Put Eq. (3) into Eq. (1) and using following formula

$$\sigma^{J}_{cc'} = \pi\lambda^2 g^J |\delta_{cc'} - U_{cc'}|^2 \tag{4}$$

Thus for fission cross sections

$$\sigma^{J}_{n,f} = \frac{\pi}{k^2} g^J \sum_{\lambda} \left[ \frac{\Gamma_{\lambda n}\Gamma_{\lambda f}}{(E_\lambda - E)^2 + (1/4)\Gamma_\lambda^2} + \sqrt{E}\frac{(1/2)u^f_\lambda \Gamma_\lambda + v^f_\lambda (E_\lambda - E)}{(E_\lambda - E)^2 + (1/4)\Gamma_\lambda^2} \right] \tag{5}$$

where

$$U^f_\lambda = \sum_{\lambda' \neq \lambda} \frac{\sqrt{(\Gamma^o_{\lambda n}\Gamma^o_{\lambda' n})}\, G^f_{\lambda\lambda'} (\Gamma_\lambda - \Gamma_{\lambda'})}{(E_\lambda - E_{\lambda'})^2 + (1/4)(\Gamma_\lambda - \Gamma_{\lambda'})^2}, \tag{6}$$

$$V^f_\lambda = \sum_{\lambda' \neq \lambda} \frac{-2\sqrt{(\Gamma^o_{\lambda n}\Gamma^o_{\lambda' n})}\, G^f_{\lambda\lambda'} (E_\lambda - E_{\lambda'})}{(E_\lambda - E_{\lambda'}) + (1/4)(\Gamma_\lambda - \Gamma_{\lambda'})^2}, \tag{7}$$

$$G^f_{\lambda\lambda'} = \sum_{c \in f} \sqrt{(\Gamma_{\lambda c}\Gamma_{\lambda' c})}. \tag{8}$$

In above equations, the first term corresponds to the single level Breit–Wigner formula, the second term expresses the contribution of the interference between levels which is represented by the two new parameters $u$ and $v$. From Eqs. (6) and (7), it is seen that the $u$ and $v$ are directly proportional to $G$ and inverse proportional to the square of the distance between levels $(E_\lambda - E_{\lambda'})^2$. $G$ contains the off–diagonal elements of $A$ which represents the contribution of interference effect between levels, therefore $u$ and $v$ are the quantities related to the interference between resonance levels. They are called interference parameters. However, the parameters $u$ and $v$ can not be calculated from the Eq. (8) because $\Gamma$ is a random quantity ($\Gamma_{\lambda f} = (2p_f)^{1/2}\gamma_{\lambda f}$) and its signs are undetermined. It is possible to determine parameters $u$ and $v$ by means of fitting experimental data in the Eq. (5) with least–squares method in case the SLBW parameters are given.

Assuming the thermal motion velocities of the target nuclei follow the Maxwell–Boltzmann distribution, using the method developed by Buckler and Pull[5,3], the Doppler broadened cross sections are given as follows :

$$\sigma^{J}_{f,m}(E,T) = \frac{4\pi}{k^2}\sqrt{(a/2m\pi)}\, g^J \sum_{\lambda} \left[ \left( \frac{\Gamma^o_{\lambda n}\Gamma_{\lambda f}}{\Gamma_\lambda} + u^f_\lambda/2 \right)\varphi^R_\lambda + (v^f_\lambda/2)\varphi^i_\lambda \right], \tag{9}$$

where

$$\varphi_\lambda^R = Re[F(\omega_1) - F(\omega_2)],$$

$$\varphi_\lambda^I = Im[F(\omega_1) - F(\omega_2)],$$

$$F(\omega) = \int_0^\infty \exp(-X^2)\frac{\omega}{X^2 + \omega^2}\,dX,$$

$$\omega_1 = \sqrt{a}\,[b + i(a - v)],$$

$$\omega_2 = \sqrt{a}\,[b + i(a + v)],$$

$$a - ib = \sqrt{(2(E_\lambda - i\Gamma_\lambda / 2) / m)},$$

$$a = M / (2kT),$$

$k$, $T$ and $v$ are the Boltzmann constant, target nucleus temperature and neutron velocity, respectively.

The Eq. (9) can be rewritten as :

$$\sigma_{f,m}^J = \sigma_{f,b}^J + \sigma_{f,int}^J , \tag{10}$$

and

$$\sigma_{f,b}^J = \frac{4\pi}{k^2}\sqrt{(a / 2m\pi)}\,g^J \sum_\lambda [(\Gamma_{\lambda n}^o \Gamma_{\lambda f}) / \Gamma_\lambda]\varphi_\lambda^R , \tag{11}$$

$$\sigma_{f,int}^J = \frac{4\pi}{k^2}\sqrt{(a / 2m\pi)}\,g^J \sum_\lambda [(u_\lambda^f / 2)\varphi_\lambda^R + (v_\lambda^f / 2)\varphi_\lambda^I]. \tag{12}$$

where $\sigma_b$ is SLBW cross section and $\sigma_{int}$ is the contribution due to the interference between resonance levels.

## 2 METHOD OF ANALYSIS

The parameters $u$ and $v$ can be determined by minimizing the quantity :

$$Q = \sum_i \omega_i |\sigma_{f,exp}(E_i) - [\sigma_{f,b}(E_i) + \sigma_{f,int}(E_i)]|^2 . \tag{13}$$

Where $\sigma_{f,exp}$ is the measured cross section, $\sigma_{f,b}$ is the SLBW cross section which are calculated by SLBW formula using the available single level parameters,

$\sigma_{f,int}$ is the trial function which contains the interference effect and $\omega_i$ stands for the statistical weights.

The least squares fit was used for $^{235}U$ fission cross section with 50 levels (1450 data points) below 30 eV.

Separating Eq. (7) into terms containing the known parameters and unknown parameters respectively, thus it is written as :

$$\sigma(E_i)=\sum_{\lambda=0}^{N_1}\sigma_{\lambda m}(E_i,u_o,v_o)+\sum_{\lambda=N_1+1}^{N_2}\sigma_{\lambda m}(E_i,u,v)+\sum_{\lambda=N_2+1}^{N}\sigma_{\lambda b}(E_i). \qquad (14)$$

Where $\sigma_{\lambda m}(E_i, u_o, v_o)$ is the contribution of the $0\rightarrow N_1$ neighboring resonances of known parameters $u_o$ and $v_o$, $\sigma_{\lambda b}(E_i)$ is the SLBW cross section of the $N_2+1\rightarrow N$ neighboring resonances and $\sigma_{\lambda m}$ is the $N_1+1\rightarrow N_2$ resonance cross sections, the parameters of which will be obtained by the least squares analysis.

The integral error of SLBW formula is defined as :

$$\delta(s)=\frac{\sum_i\sigma_{f,b}(E_i)\Delta E_i-\sum_i\sigma_{f,exp}(E_i)\Delta E_i}{\sum_i\sigma_{f,exp}(E_i)\Delta E_i}100\%. \qquad (15)$$

In general, $\delta(s)$ for SLBW is just 6~7%. It shows that the interference effect between levels is small. Since the parameters $(u,v)$ are very small, $u$ and $v$ obtained by least squares fitting are unsatisfactory. The integral error of the correction cross section $\delta(m)$ is

$$\delta(m)=\frac{\sum_i\sigma_{f,m}(E_i)\Delta E_i-\sum_i\sigma_{f,exp}(E_i)\Delta E_i}{\sum_i\sigma_{f,exp}(E_i)\Delta E_i}100\%. \qquad (16)$$

Notice that the relationship between interference parameters $(u,v)$ and cross sections is linear. A simple modified method is advancd in order to obtain the optimum $u$ and $v$. Assuming that $\sigma_{f,m}-\sigma_{f,exp}\neq 0$, where $\sigma_{f,m}=\sigma_{f,b}+\sigma_{f,int}$ and $\sigma_{f,int}$ is the interference cross section calculated by using of parameters $u$ and $v$, which were obtained by using least squares fitting.

Soppose

$$K=\frac{\sigma_{f,b}-\sigma_{f,exp}}{\sigma_{f,exp}-\sigma_{f,m}}, \tag{17}$$

thus

$$\sigma_{f,exp}-[\sigma_{f,b}+\sigma_{f,m}(u,v)]=(1/K)[\sigma_{f,b}-\sigma_{f,exp}],$$

or

$$\sigma_{f,int}(u,v)=[(K+1)/K](\sigma_{f,exp}-\sigma_{f,b}). \tag{18}$$

The aim of modifying the parameters is to obtain new parameters $u'$ and $v'$, in so much that

$$\sigma_{f,exp}-[\sigma_{f,b}+\sigma_{f,int}(u',v')]=0,$$

therefore

$$\sigma_{f,int}(u',v')=\sigma_{f,exp}-\sigma_{f,b}.$$

By virtue of Eq. (18), thus

$$\sigma_{f,int}(u',v')=[K/(K+1)]\sigma_{f,int}(u,v).$$

Since the relationship between $\sigma_{f,int}$ and parameters $u$ and $v$ is linear, we can obtain

$$u'_\lambda=[K/(K+1)]u_\lambda,$$

$$v'_\lambda=[K/(K+1)]v_\lambda.$$

The new parameters $u'$ and $v'$ will improve the "goodness of fitting". Actually in the calculation we used the average modified coefficient $K$ of the $j$–th resonance, which is obtained from some choosen data points; the satisfactory interference parameters can be obtained by iterative procedure.

It should be shown that the result of the modifying $u$ and $v$ to reduce integral error $\delta$(m) is agreement with minimizing $Q$ in least squares fitting.

The program CBWFIT has been written for analysing low energy neutron fission cross section of fissile elements with FORTRAN 77.

The program can output the integral error of each iterative procedure in order to know the changes of the error in modification process.

The program can be used to calculate the corrected cross sections with artificial adjusted parameters in order to investigate the effects of $u$ and $v$ to the cross section.

# 3 RESULTS

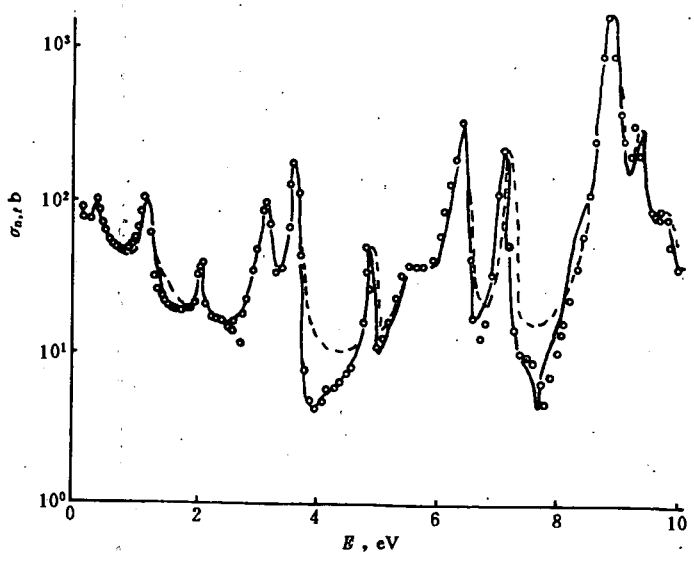


Fig. 1 Comparison of fission cross sections below 10 eV

ooo Experimental data

--- SLBW calculation

—— Multilevel correction

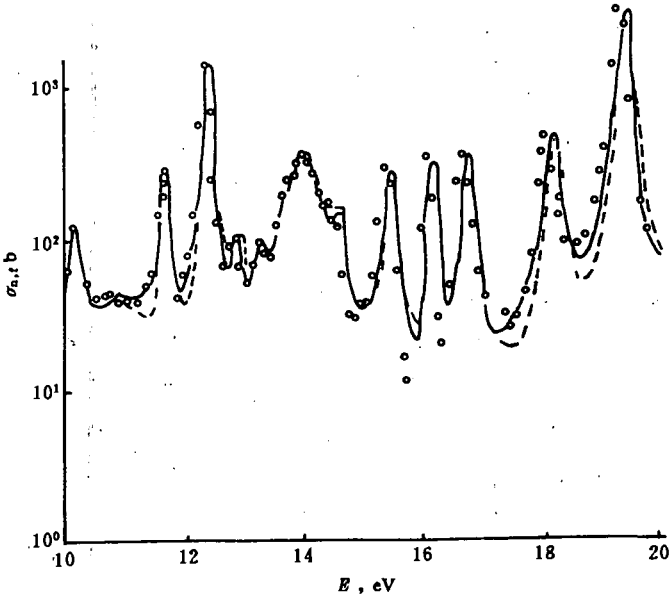


Fig. 2 Comparison of fission cross sections from 10 to 20 eV

ooo Experimental data

--- SLBW calculation

—— Multilevel correction

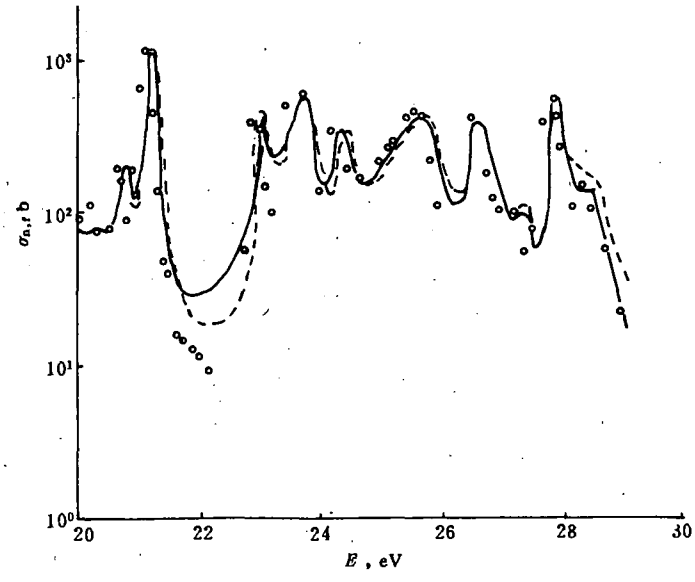


Fig. 3 Comparison of fission cross section from 20 to 30 MeV

ooo Experimental data

--- SLBW calculation

—— Multilevel correction

The least squares fitting were performed for $^{235}U$ with 50 levels below 30 eV. The experimental data were obtained in energy range of below 0.4 eV from AEEW–M502 (1964), 0.4 to 8 eV from Ref. [6] and 8 to 30 eV from Ref. [7]. The single level parameters were obtained from Ref. [8].

The obtained parameters $(u,v)$ and the single level parameters are shown in Table 1. The comparisons between the measured values, the SLBW cross sections and the modified cross sections are shown in Figs. 1, 2 and 3.

The comparisons between $\delta(s)$ of the SLBW cross sections and $\delta(m)$ of modified cross sections obtained in the present work are shown in Table 2.

It follows from the above mentioned that the corrected formula is better than SLBW in reproducing the measured fission cross section. $\delta(m)$ obtained in present work is less than 1%, therefore, the corrected formula is successful at a new attempt to get the multilevel formula results by a simple way.

The authors would like to acknowledge Profs. Zhou Delin and Zhuang Youxiang, from China Institute of Atomic Energy, for many helpful discussions.

**Table 1 Single level parameters of $^{235}U$ used for present calculation and obtained interference parameters**

| $E_\lambda$, eV | $\Gamma_n^\circ$, eV | $\Gamma_\gamma$, eV | $\Gamma_v$, eV | $u_t$, $eV^{1/2}$ | $v_t$, $eV^{1/2}$ |
|---|---|---|---|---|---|
| −0.14900+1 | 0.30164−2 | 0.20700+0 | 0.23768+0 | −0.40764−3 | 0.183889−4 |
| 0.29000+0 | 0.56000−5 | 0.99000−1 | 0.13500+0 | 0.33899−6 | 0.11405 −6 |
| 0.11400+1 | 0.14200−4 | 0.11620+0 | 0.15082+0 | −0.14593−5 | 0.45659 −5 |
| 0.20310+1 | 0.53700−5 | 0.98140−2 | 0.44696−1 | −0.80128−7 | −0.71546 −7 |
| 0.29200+1 | 0.28400−5 | 0.20000+0 | 0.22000+0 | 0.15063−6 | 0.34755 −5 |
| 0.31470+1 | 0.12630−4 | 0.10637+0 | 0.13961+0 | −0.20178−5 | −0.99059 −6 |
| 0.36090+1 | 0.24000−4 | 0.50637−1 | 0.84379−1 | −0.30636−5 | −0.98619 −5 |
| 0.48480+1 | 0.27410−4 | 0.35870−2 | 0.39592−1 | −0.16899−6 | −0.12998 −5 |
| 0.54480+1 | 0.14400−5 | 0.30117−1 | 0.90120−1 | 0.29077−7 | −0.19076 −6 |
| 0.56000+1 | 0.14080−4 | 0.62189+0 | 0.64192+0 | 0.41486−5 | 0.98340 −5 |
| 0.62100+1 | 0.25600−4 | 0.18736+0 | 0.23090+0 | −0.40697−5 | 0.16422 −4 |
| 0.63820+1 | 0.10622−3 | 0.95480−2 | 0.44788−1 | −0.17946−4 | −0.18505 −4 |
| 0.70770+1 | 0.47590−4 | 0.28233−1 | 0.63934−1 | −0.63542−5 | −0.12582 −4 |
| 0.87810+1 | 0.37910−3 | 0.91000−1 | 0.12329+0 | −0.26357−4 | −0.31061 −4 |
| 0.92860+1 | 0.53700−4 | 0.75000−1 | 0.11076+0 | 0.20478−5 | −0.48707 −5 |
| 0.97300+1 | 0.17000−4 | 0.23700+0 | 0.26905+0 | 0.33443−5 | −0.11655 −5 |
| 0.10180+2 | 0.19400−4 | 0.62500−1 | 0.10056+0 | 0.15262−5 | 0.89245 −7 |
| 0.10800+2 | 0.28400−4 | 0.86800+0 | 0.93509+0 | −0.90177−5 | 0.16334 −4 |
| 0.11666+2 | 0.18370−3 | 0.62500−2 | 0.47277−1 | −0.84719−5 | −0.42608 −5 |
| 0.12396+2 | 0.35850−3 | 0.27500−1 | 0.63262−1 | −0.18580−4 | −0.23609 −4 |
| 0.12861+2 | 0.14800−4 | 0.86000−1 | 0.11955+0 | 0.31020−5 | −0.69331 −5 |
| 0.13275+2 | 0.10800−4 | 0.12280+0 | 0.15144+0 | 0.16786−5 | −0.24994 −5 |
| 0.13700+2 | 0.10000−4 | 0.93500−1 | 0.12394+0 | 0.44544−5 | −0.41619 −5 |
| 0.13996+2 | 0.14360−3 | 0.47000+0 | 0.49654+0 | 0.69456−5 | −0.11928 −5 |
| 0.14544+2 | 0.30200−4 | 0.20900−1 | 0.56215−1 | −0.12968−5 | −0.48885 −6 |
| 0.15406+2 | 0.60400−4 | 0.43300−1 | 0.78837−1 | −0.23262−5 | −0.44857 −5 |
| 0.16088+2 | 0.90000−4 | 0.18617−1 | 0.50361−1 | −0.26437−5 | −0.52169 −5 |
| 0.16667+2 | 0.66870−4 | 0.10089+0 | 0.13327+0 | 0.19556−5 | −0.75824 −5 |
| 0.18052+2 | 0.90500−4 | 0.12500+0 | 0.16038+0 | −0.24786−5 | −0.12622 −6 |
| 0.18960+2 | 0.26000−4 | 0.55000−1 | 0.10512+0 | 0.11926−5 | 0.30682 −4 |
| 0.19297+2 | 0.72700−3 | 0.60179−1 | 0.98194−1 | −0.11772−3 | −0.97322 −4 |
| 0.20130+2 | 0.19550−4 | 0.22609+0 | 0.24009+0 | 0.68771−7 | −0.15148 −5 |
| 0.20200+2 | 0.29000−5 | 0.72000−3 | 0.50013−1 | 0.68656−6 | 0.44747 −5 |
| 0.20610+2 | 0.42110−4 | 0.43515−1 | 0.84191−1 | −0.25603−5 | 0.97855 −6 |
| 0.21072+2 | 0.32736−3 | 0.31658−1 | 0.73503−1 | −0.11219−4 | −0.14072 −4 |

| | | | | | |
|---|---|---|---|---|---|
| 0.22939+2 | 0.91000−4 | 0.42330−1 | 0.75436−1 | −0.20497−4 | −0.11372 −4 |
| 0.23412+2 | 0.14544−3 | 0.50000−2 | 0.32204−1 | −0.44614−5 | −0.10400 −4 |
| 0.23629+2 | 0.17605−3 | 0.18200+0 | 0.22586+0 | −0.19830−4 | −0.35423 −4 |
| 0.24245+2 | 0.54500−4 | 0.27000−1 | 0.58268−1 | −0.14387−4 | −0.29580 −4 |
| 0.24370+2 | 0.30300−4 | 0.65000−1 | 0.10015+0 | 0.13040−4 | −0.12256 −5 |
| 0.25200+2 | 0.13471−3 | 0.82500+0 | 0.85068+0 | 0.38963−4 | −0.57283 −4 |
| 0.25590+2 | 0.11160−3 | 0.36000+0 | 0.38556+0 | −0.95190−5 | −0.18702 −4 |
| 0.26480+2 | 0.92500−4 | 0.16000+0 | 0.19248+0 | −0.10805−5 | −0.24830 −4 |
| 0.26740+2 | 0.16570−4 | 0.22000+0 | 0.25009+0 | 0.33743−4 | 0.13669 −4 |
| 0.27149+2 | 0.16340−4 | 0.73500−1 | 0.11559+0 | −0.97880−6 | 0.24328 −5 |
| 0.27796+2 | 0.12793−3 | 0.88000−1 | 0.12067+0 | −0.43040−5 | −0.96847 −5 |
| 0.28090+2 | 0.58800−5 | 0.25000−1 | 0.65031−1 | 0.14383−4 | −0.89453 −5 |
| 0.28351+2 | 0.35410−4 | 0.11730+0 | 0.14919+0 | 0.11940−5 | 0.49389 −7 |
| 0.28710+2 | 0.84000−5 | 0.80000−1 | 0.13004+0 | 0.10314−5 | 0.77889 −6 |
| 0.29644+2 | 0.32590−4 | 0.24000−1 | 0.61177−1 | 0.17552−5 | −0.23071 −5 |
| 0.30590+2 | 0.41100−4 | 0.10990+0 | 0.15523+0 | | |
| 0.30680+2 | 0.95830−4 | 0.18731−1 | 0.54532−1 | | |
| 0.32070+2 | 0.32197−3 | 0.60276−1 | 0.99823−1 | | |
| 0.33520+2 | 0.22117−3 | 0.23139−1 | 0.56859−1 | | |
| 0.34370+2 | 0.38425−3 | 0.41840−1 | 0.87253−1 | | |
| 0.34850+2 | 0.18595−3 | 0.76753−1 | 0.11610+0 | | |
| 0.35187+2 | 0.59010−3 | 0.68598−1 | 0.10350+0 | | |
| 0.35300+2 | 0.26383−3 | 0.65000+0 | 0.69157+0 | | |

**Table 2 Comparison of the integral error**

| energy range | $\delta(s)$ | $\delta(m)$ |
|---|---|---|
| 0 − 1.8 eV | 0.85 % | 0.01 % |
| 1.8 − 8 eV | 7.3 % | 0.49 % |
| 8 − 17.4 eV | 4.7 % | 0.87 % |
| 17.4 − 30 eV | 4.4 % | 0.49 % |

## REFERENCES


[1] Qiu Guochun, Lu Guoxiong, Neutron resonance theory and neutron resonance parameter, p.1 (1981) (in Chinese).

[2] H. Takano, Y. Ishiguro, J. Nucl. Sci. Technol., 14(9), 627(1977).

[3] H. Takano, K. Kobayashi, JAER-M-4999(1972).

[4] E. Vogt, Phys. Rev., 112 203(1958).

[5] P. A. C. Buckler and I. C. Pull, AEEW-R226(1962).

[6] G. de Saussure et al., ORNL-TM-1804(1967).

[7] R. B. Perez et al., ORNL-TM-3696(1972).

[8] J. R. Smith, R. C. Young, ANCR-1044(1971).

# CINDA INDEX

| Nuclide | Quantity | Energy (eV) | | Lab | Type | Documentation | | | |
|---|---|---|---|---|---|---|---|---|---|
| | | Min | Max | | | Ref | Vol | page | Date |
| D | Elastic | 1.05 | 2.0+7 | FUD | Theo | Jour CNDP | 4 | 26 | Nov 90 |
| | (n,2n) | 3.4+6 | 2.0+7 | AEP | Eval | Jour CNDP | 4 | 41 | Nov 90 |
| $^{7}$Li | Diff Elastic | 7.0+6 | 2.0+7 | JIL | Theo | Jour CNDP | 4 | 7 | Nov 90 |
| | Diff Inelastic | 7.0+6 | 2.0+7 | JIL | Theo | Jour CNDP | 4 | 7 | Nov 90 |
| $^{10}$B | (n,α) | 4.0+3 | | TSI | Theo | Jour CNDP | 4 | 20 | Nov 90 |
| $^{16}$O | Total | 1.0−5 | 6.2+6 | TSI | Theo | Jour CNDP | 4 | 16 | Nov 90 |
| | (n,n) | 1.0−5 | 6.2+6 | TSI | Theo | Jour CNDP | 4 | 16 | Nov 90 |
| | (n,α) | 1.0−5 | 6.2+6 | TSI | Theo | Jour CNDP | 4 | 16 | Nov 90 |
| | Polarization | | 2.6+6 | TSI | Theo | Jour CNDP | 4 | 20 | Nov 90 |
| $^{23}$Na | (n,γ) | 1.0−5 | 2.0+7 | AEP | Eval | Jour CNDP | 4 | 33 | Nov 90 |
| Cr | Diff Elastic | 1.5+7 | | TSI | Expt | Jour CNDP | 4 | 3 | Nov 90 |
| Fe | Diff Elastic | 1.5+7 | | TSI | Expt | Jour CNDP | 4 | 3 | Nov 90 |
| $^{59}$Co | (n,γ) | 1.0−5 | 2.0+7 | AEP | Eval | Jour CNDP | 4 | 45 | Nov 90 |
| Ni | Diff Elastic | 1.5+7 | | TSI | Expt | Jour CNDP | 4 | 3 | Nov 90 |
| $^{235}$U | (n,f) | 3.0+4 | 2.0+7 | AEP | Eval | Jour CNDP | 4 | 49 | Nov 90 |
| $^{238}$U | (n,γ) | 3.0+4 | 2.0+7 | AEP | Eval | Jour CNDP | 4 | 49 | Nov 90 |
| | (n,f) | 3.0+4 | 2.0+7 | AEP | Eval | Jour CNDP | 4 | 49 | Nov 90 |
| $^{239}$Pu | (n,f) | 3.0+4 | 2.0+7 | AEP | Eval | Jour CNDP | 4 | 49 | Nov 90 |

| Author, Comments |
| --- |
| Chen Jianxin+ PHASE SHIFT ANALYSIS, CS. |
| Cai Dunjiu+ FOR CENDL-2. |
| Zhu Yaoyin+ OPTMDL, DWBA, ANGDIS. |
| Zhu Yaoyin+ OPTMDL, DWBA, ANGDIS. |
| Chen Zhenpeng+ R MATRIX ANALYSES, ANGDIS. |
| Chen Zhenpeng+ R MATRIX ANALYSIS, CS. |
| Chen Zhenpeng+ R MATRIX ANALYSIS, CS. |
| Chen Zhenpeng+ R MATRIX ANALYSIS, CS. |
| Chen Zhenpeng+ R MATRIX CALC, POLRZD (ANG). |
| Yuan Hanrong CS. |
| Qi Huiquan+ PASS D, ANGDIS. |
| Qi Huiquan+ PASS D, ANGDIS. |
| Liu Tong+ CS. |
| Qi Huiquan+ PASS D, ANGDIS. |
| Liu Tingjin+, SIMULTANEOUS EVAL, CS, COV. |
| Liu Tingjin+, SIMULTANEOUS EVAL, CS, COV. |
| Liu Tingjin+ SIMULTANEOUS EVAL, CS, COV. |
| Liu Tingjin+, SIMULTANEOUS EVAL, CS, CON. |

核数据进展通讯
原子能出版社出版
(北京 2108 信箱)
中国核数据中心激光照排
北京市海淀区三环快速印刷厂印刷
☆
开本 787×1092 1/16 · 印张 2 字数 60 千字
1991 年 5 月北京第一版 · 1991 年 5 月第一次印刷
ISBN7-5022-0442-3
TL-229

ISBN 7-5022-0442-3

TL-229